Ore Geology Reviews 106 (2019) 176–191

Contents lists available at ScienceDirect

Ore Geology Reviews

journal homepage: www.elsevier.com/locate/oregeorev

Spatial distribution of sulfur isotope ratios associated with the Eagle Ni-Cu sulfide deposit in Upper Peninsula, Michigan: Implications on country-rock contamination in a dynamic magma conduit

Joyashish Thakurta[a,*,1], Benjamin Hinks[a,b], Katharine Rose[a]

[a] Department of Geological and Environmental Sciences, Western Michigan University, Kalamazoo, MI, USA
[b] Department of Environmental Quality, State of Michigan, USA

A B S T R A C T

The Eagle Ni-Cu magmatic sulfide deposit in the Upper Peninsula of Michigan is hosted in mafic-ultramafic rocks associated with the 1.1 Ga Midcontinent Rift event. The deposit consists of massive, semi-massive and disseminated sulfide textural zones located in two closely spaced funnel-shaped intrusive bodies, called the Eagle and Eagle East intrusions. The intrusions are surrounded by metamorphosed supracrustal Paleoproterozoic rocks of the Michigamme Formation and at depth by a Neoarchean migmatitic banded gneiss. $\delta^{34}S$ values were obtained from sulfide minerals separated by micro-drilling from different parts of the intrusions and the surrounding rocks. The $\delta^{34}S$ values from the intrusions cluster within a small range between 1 and 3‰ relative to V-CDT regardless of the mode of occurrence, textural type, mineral type and location of the sample. However, disseminated sulfide minerals in the metasedimentary country rocks of the Michigamme Formation show a substantially greater range in $\delta^{34}S$ values between 4 and 35‰ with a median of 7.7‰ while disseminated sulfides in the basement granite-gneiss show values ranging from −9 to 13‰ with a median of 2.5‰. The narrow range of $\delta^{34}S$ values within the intrusions despite wide variabilities in the surrounding country rocks can be explained by the incorporation of crustal sulfur by a mantle-derived magma, followed by a homogeneous mixing of the immiscible sulfide liquid, with a silicate liquid to sulfide liquid ratio (R-factor) of 200 or more. The assimilation of crustal rocks and the mixing of the resultant immiscible sulfide liquid must have been facilitated by the rapid movement of magma along a narrow conduit system.

1. Introduction

Contamination of magma by country rock has been recognized as an important step in the formation of some economic magmatic Cu-Ni-PGE sulfide mineral deposits (Li and Ripley, 2005; Ripley and Li, 2003, 2013; Naldrett, 2004; Keays and Lightfoot, 2010). Sulfide saturation in a mantle-derived mafic magma depends on the sulfur content and the degree of sulfide solubility. Experimental studies by Buchanan and Nolan (1979) and Mavrogenes and O'Neil (1999) on the temperature and pressure dependence of sulfide saturation indicate that at shallow crustal levels a mantle-derived basaltic magma can never attain sulfide saturation unless it undergoes high degree of fractional crystallization or assimilates a large quantity of crustal rocks. Country rock assimilation can potentially introduce external sulfur from crustal rocks into the magmatic system which could lead to sulfide saturation (Ripley and Li, 2013). Moreover, assimilation of siliceous (Lightfoot and Hawkesworth, 1997) and carbonate country rocks (Lehmann et al., 2007) could decrease the sulfide solubility of a mafic magma, which might also lead to sulfide saturation. Robertson et al. (2015) proposed that the liberation and assimilation of sulfur from country rocks can be achieved by the production of sulfurous fluids from the country rocks into the magma as well as by direct melting of wall rocks and xenoliths. Sulfur isotope ratio has been used as a useful geochemical tool to ascertain the degree and nature of assimilation of external sulfur (Ripley and Li, 2003; Holwell et al., 2007; Ripley et al., 2010; Maier et al., 2010; Fiorentini et al., 2012; Ripley and Li, 2013; Hughes et al., 2016).

Upon the attainment of sulfide saturation, tiny dispersed droplets of immiscible Fe-Ni-Cu sulfide liquid appear in the magma (Robertson et al., 2016). The collection and amalgamation of these metallic sulfide droplets is an important process for the formation of economic Ni-Cu-PGE sulfide mineral deposits, although the mechanism of aggregation of this sulfide liquid is poorly understood. There are uncertainties with respect to the location or depth of sulfide input from the country rocks into a magmatic system (Lesher, 2018). Additionally, the proportions of crustal- and mantle-derived sulfur in these deposits have been debated frequently (Ripley et al., 2002; Lehmann et al., 2007; Seat et al., 2009; Keays and Lightfoot, 2010). In this work, the sulfur isotope ratio, $\delta^{34}S$, was used to address the extent of sulfur input from country rocks into magma flowing through a conduit at the Eagle Ni-Cu sulfide deposit in the Upper Peninsula of Michigan, USA.

* Corresponding author.
E-mail address: joyashish.thakurta@wmich.edu (J. Thakurta).
[1] ORCID ID: 0000-0001-9867-3542.

https://doi.org/10.1016/j.oregeorev.2019.01.008
Received 8 October 2018; Received in revised form 31 December 2018; Accepted 10 January 2019
Available online 11 January 2019
0169-1368/

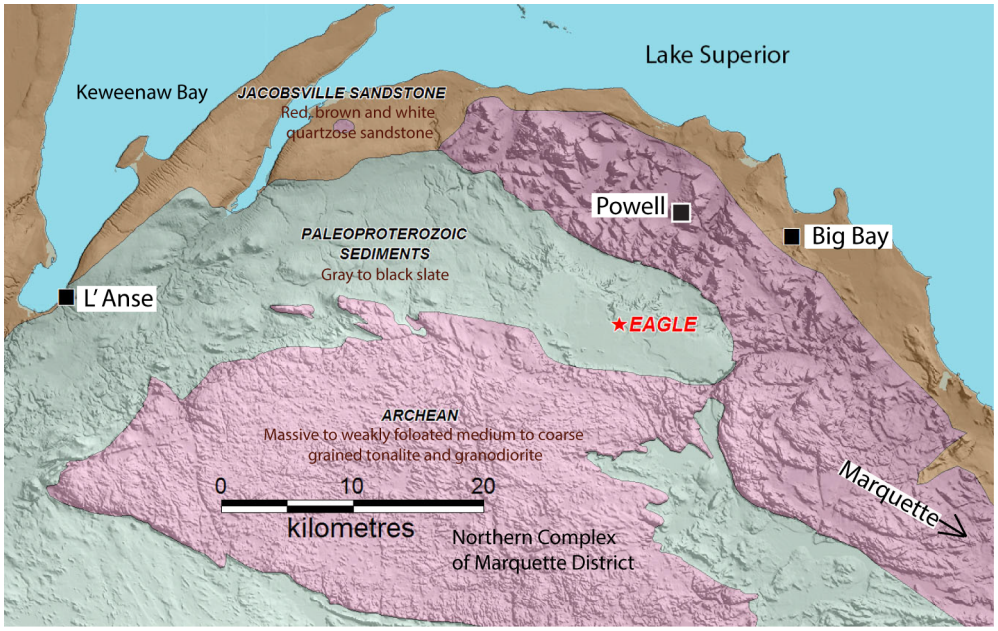

Fig. 1a. Location of the Eagle deposit in the Great Lakes Region of Upper Peninsula Michigan and the known occurrences of associated country rocks (Sims, 1992; Rossell and Coombes, 2005).

Ding et al. (2012) addressed various aspects of country rock contamination of the Eagle deposit using Os, Nd, O and S isotopes. From the $\delta^{34}S$ values between 0.3 and 4.6‰ in the sulfide mineral deposit and values up to 29‰ in the adjacent country rocks, they concluded that the sulfur isotope ratios observed in the sulfide deposit cannot be explained by a simple mixing model between magmatic sulfur and sulfur from the immediate country rocks. They proposed that sulfur must have been added to the magma from multiple sources. This work continues the investigation on country rock contamination of the Eagle deposit in terms of sulfur isotope signatures and examines the mechanism of the addition of external sulfur into the magma in a dynamic conduit system based on the spatial distribution of sulfur isotope ratios in sulfide minerals within the Eagle deposit, relative to the surrounding country rocks.

1.1. The Eagle deposit and its geologic setting

The Eagle intrusion is located in the north central portion of Michigan's Upper Peninsula within Michigamme Township, Marquette County. It is approximately 14 km south west from the town of Big Bay and 40 km north west from Marquette (Fig. 1a). The Eagle deposit has an overall length of ~480 m, width of ~100–200 m, and a vertical extension of more than 300 m, while the Eagle East intrusion is ~600 m long, ~150 m wide, and > 500 m deep (Ding et al., 2010). The Eagle deposit has been mined since 2014 and it is expected to produce around 4.6 million metric tons of ore during an estimated lifetime of seven years, with an average grade of 3.7% Ni, 3.1% Cu, 0.10% Co, 0.3 ppm Au, 0.9 ppm Pt, and 0.7 ppm Pd (Clow et al., 2017).

The Eagle East intrusion is located about 600 m east of the Eagle Intrusion. The Eagle East sulfide intrusion is regarded as a possible feeder dike for the main Eagle intrusion although the precise petrogenetic and structural relationships between these intrusions have remained obscure. In 2016, Lundin Mining announced the discovery of a high-grade Ni-Cu sulfide deposit at the base of the Eagle East intrusion (Lundin Mining, 2016) with 1.18 million metric tons of sulfide ore showing an average grade of 5.2% Ni and 4.3% Cu. Both Eagle and Eagle East intrusions have conical cross-sections with narrow feeder conduits underneath (Fig. 2).

Country rocks near the Eagle and Eagle East intrusions are Proterozoic low grade metamorphosed sedimentary and felsic volcanic rocks and Archean granite-gneiss (Johnson and Bornhorst, 1991; Sims et al., 1993). These Archean basement rocks are divided into two terranes, referred to as the Northern and Southern Complexes. The Northern Complex (Wawa sub-province), where the Eagle intrusion is located, is composed of granite-greenstone rocks dated between 2700 Ma and 2900 Ma (Sims et al., 1993; Tohver et al., 2007). The Southern Complex (Minnesota River Valley sub-province) is composed of gneiss, migmatite, and amphibolite which were intruded by late Archean granites (Sims et al., 1993; Tohver et al., 2007). The oldest gneissic rock in the region has been dated between 2600 and 3400 Ma (Van Schmus and Woolsey, 1975; Peterman et al., 1980).

The boundary separating the Archean and Proterozoic complexes is known as the Great Lakes Tectonic Zone (GLTZ). The GLTZ is a large, regional paleo-suture zone resulting from continent-continent collision thought to have occurred between 2692 and 2686 Ma (Schneider et al., 2002). It is a 1000 km long boundary that extends from Marquette, MI into Wisconsin and Minnesota and eastward into New York. Sims (1991) proposed a northwestward direction of tectonic movement along the GLTZ and inferred that the Northern Complex was most likely overridden by the Southern Complex. The Archean rocks in northern Michigan are covered by sedimentary deposits of the Early Proterozoic Marquette Range Supergroup. These meta-sedimentary rocks can be found in the Marquette synclinorium, the Republic trough, the Dead River basin, the Clark Creek basin, and the Baraga basin (Sims, 1991).

The surficial outcrops of the Eagle and Eagle East intrusions are known as Yellow Dog Peridotite which are located within the Baraga basin. The Baraga basin, which covers an area of approximately 400 km^2, is a structural trough filled with shelf sediments of the Baraga Group formed during the ~1.85 Ga Penokean Orogeny (Van Schmus et al., 1987). Lithologies, from the bottom to the top consist primarily of a thin quartzite unit, named the Goodrich quartzite, a 15–30 m thick chert-carbonate unit, which is correlated with the Greenwood Iron Formation, and a graywacke-slate member of the Michigamme Formation (Ding et al., 2012). The Baraga basin is thought to have formed as a fore-deep basin during the collision of the Archean Superior craton with the Pembine-Wausau volcanic-arc terrane. This is known to have occurred during the Penokean Orogeny as a south-facing subduction zone or as a back-arc basin deposit which formed behind a north facing

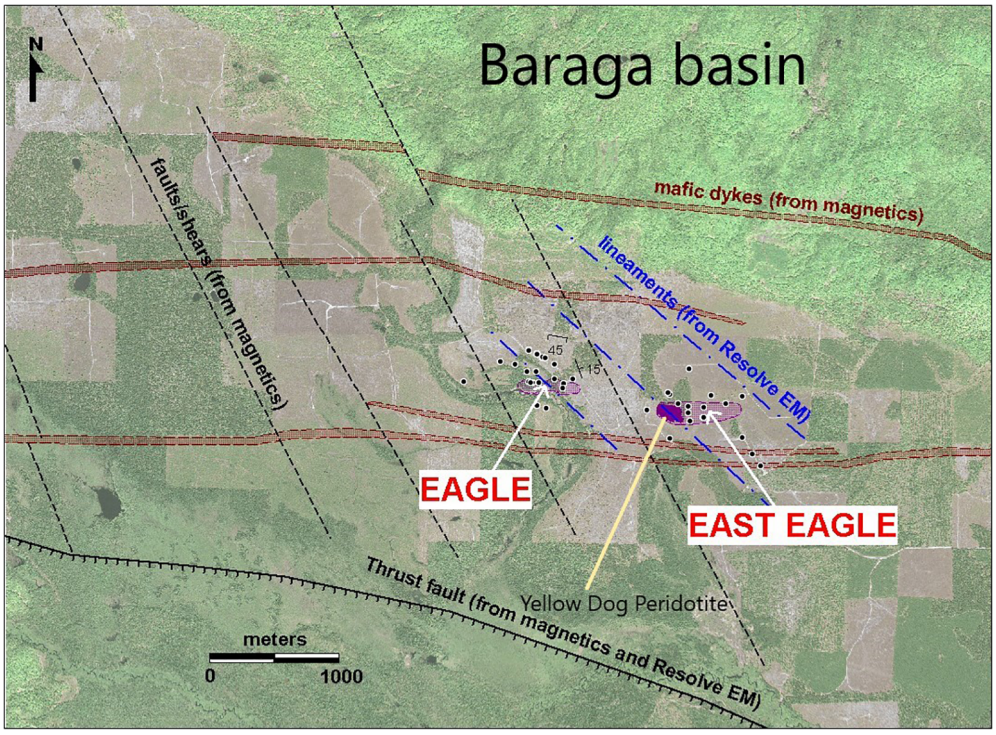

Fig. 1b. Close-up map view of the Eagle and Eagle East deposits (Rossell and Coombes, 2005).

subduction zone (Schneider et al., 2002). The Penokean convergence started by 1875 Ma and was completed by 1835 Ma; (Schneider et al., 2002; Schulz and Cannon, 2007).

The Eagle and Eagle East intrusions are parts of the east-west trending Marquette-Baraga dike swarm associated with early stages of ~1.1 Ga Midcontinent Rift System (MRS) magmatism (Fig. 1b; Ding et al., 2010; Ripley 2015). The MRS is a prominent, failed divergent spreading center that extends through central Michigan towards Lake Superior and curves southwest towards Kansas (Van Schmus and Hinze, 1985; Nicholson et al., 1997; Stein et al., 2018). Both the Eagle and Eagle East bodies formed as intrusive dikes which penetrated through the Baraga basin sediments (Ding et al., 2010, 2011). The age of the Eagle intrusion, determined by the U-Pb baddeleyite method, has been found to be 1107.3 ± 3.7 Ma which constrains its origin in the early stages of formation of the MRS (Ding et al., 2010).

2. Methods

2.1. Sampling

Samples of the sulfide-mineralized intervals along with the mafic-ultramafic host rocks of the Eagle and Eagle East deposits, surrounding Paleoproterozoic meta-sedimentary country rocks, and Archean granitic basement rocks were collected from the Eagle Mine core repository in Ishpeming, MI. Two hundred sixty one samples from 32 drill cores were collected from the Eagle intrusion and Eagle East intrusion,

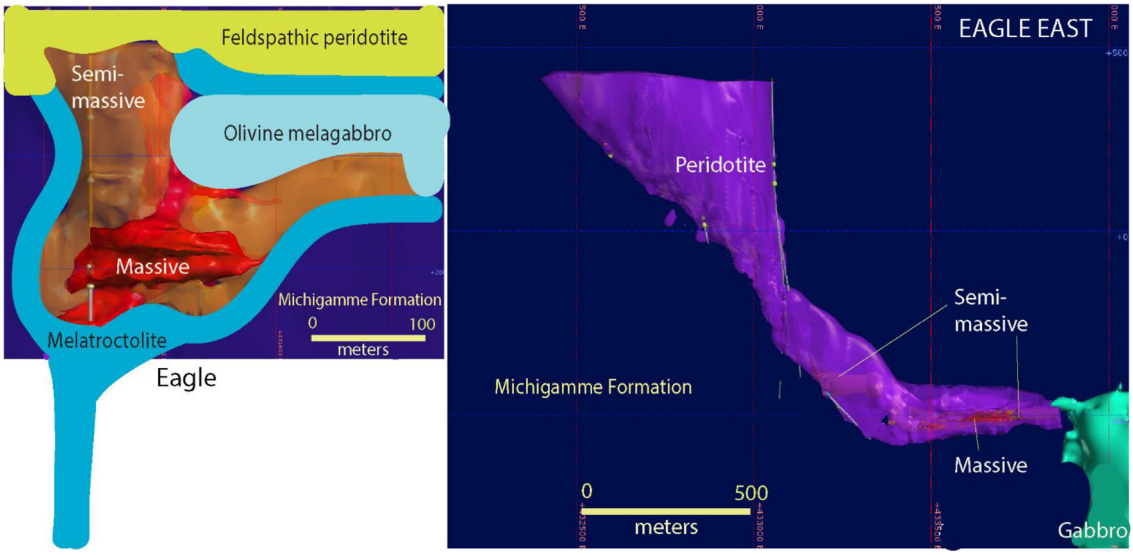

Fig. 2. Schematic 3D views of the Eagle and Eagle East intrusions looking north. The funnel shaped upper part and narrow conduits underneath have been delineated by exploratory drilling (Modified from Ding et al., 2010; Clow et al., 2017).

Table 1
List of drill core samples used in the study.

Rock types/locations	Drill hole	Number of samples
Eagle	EAUG0011	18
	EAUG0012	7
	04EA083	8
	04EA054	18
	12EA269	9
	04EA073	9
	EUGX0007	8
	12EA273A	16
	03EA032	8
	EAUG0300	13
	EAUG0301	10
East Eagle	EUGX0035	7
	EUGX0040	11
	14EA331G	8
	14EA331H	11
	14EA331I	16
	08EA222A	3
	08EA222C	3
	08EA222D	10
Proterozoic country rocks	DL-1	3
	DL-3b	2
	DL-4	7
	DL-5	3
	DL-7	5
	LY-1	1
	17EA360D	8
	17EA364	7
Archean basement rocks	08EA183	6
	08EA184	8
	12EA315	3
	12EA296A	12
	17EA360A	3

as listed in Table 1. Sample selection was based on the modal content and textural types of sulfide minerals in the intrusions and in the surrounding country rocks as listed in the supplementary Table S1. Samples were collected to represent most parts of intrusion and contact regions with country rocks based on the availability of drill cores. Key characteristics examined in thin sections include: mineralogy, texture, alteration products, and relationship of the sulfides with surrounding groundmass. Contacts of disseminated, semi-massive, and massive sulfides were also examined to determine the relationship of the sulfides with peridotite and sedimentary country rocks. Photomicrographs of thin sections were taken with a Leica microscope, and a "LAS EZ Application Suite" was used to capture images of sulfide textures and mineralogy.

2.2. Sulfur isotope analysis

Sulfur isotope ratios were determined from drill core samples of sulfide minerals collected from the ore bodies, the intrusive igneous rocks, the surrounding meta-sedimentary country rocks and the granitic basement rocks. Samples were selected for isotope analysis based on the following factors: 1. Spatial locations determined with respect to drill core orientations and depths; 2. Textural types of sulfide minerals which include disseminated, semi-massive and massive; 3. Types of host rocks of the sulfide minerals such as, the peridotite intrusion, siltstone/slate, contact metamorphosed hornfelsic slate, graphite-bearing graywacke, and granite-gneiss.

The sulfide minerals from selected rock samples were drilled out as fine powder using a micro Dremel hand-operated drilling tool. In most instances sample powder was carefully drilled out from a single mineral type, such as pyrrhotite and chalcopyrite. However, in samples with small grain size and patchy aggregates of multiple sulfide minerals, some degree of mixing between two or more sulfide minerals might have taken place. Approximately 0.1–0.2 mg of powdered sulfide mineral samples were then weighed in a Sartorius microbalance and placed into 3.5 × 5 mm tin capsules. Samples are then mixed with approximately 0.2 mg of V_2O_5 flux inside the tin capsules. These tin capsules are loaded into the sample carousel of a Costech elemental analyzer for combustion at 980 °C. The SO_2 gases released were analyzed (Studley et al., 2002) by a Delta-V continuous-flow Isotope Ratio Mass-spectrometer (IRMS) at the Stable Isotope laboratory in Western Michigan University. The obtained $\delta^{34}S$ values were reported with respect to the "Vienna Canyon Diablo Troilite" (V-CDT) standard with a $\delta^{34}S$ value of 0‰. The $\delta^{34}S$ values of samples were calculated by the formula:

$$\delta^{34}\,S = (({}^{34}S/{}^{32}S_{sample} - {}^{34}S/{}^{32}S_{standard}) \div ({}^{34}S/{}^{32}S_{standard})) \times 1000\%.$$

The international sulfur isotope reference standards used in the analyses were IAES-S-1 with a $\delta^{34}S$ value of −0.3‰ and IAEA-S-2 with a $\delta^{34}S$ value of 21.7‰.

Raw sample values were corrected using a multiple-point linear normalization method. For the six sample runs, this normalization method yielded sample-standard correlation lines with R^2 values of 0.99 or more. The equations produced by these trend lines were used to correct the values relative to V-CDT. The sample reproducibility was ± 0.2‰ or better.

3. Results

3.1. Rock types

The major rock types used in this study are described below. Detailed descriptions of rock types at Eagle and Eagle deposits have also been reported by Ding et al. (2010). Additional information about most samples used in this study, in point-by-point locations along drill cores, can be seen in supplementary Table S1.

3.1.1. Ultramafic-mafic rocks

Ding et al. (2010) proposed four ultramafic-mafic intrusive rock types at Eagle: feldspathic peridotite, feldspathic pyroxenite, melatroctolite, and olivine melagabbro. Collectively these group of rocks contain 20–50% olivine, 5–15% clinopyroxene, 15–40% orthopyroxene, and 15–20% plagioclase by volume. These rocks represent a gradational, ultramafic-mafic cumulate sequence with no visible boundaries. This is indicative of a continuous and sequential separation of the above minerals from a fractionating magma. Mosaic-type adcumulate texture is often seen among olivine, clinopyroxene and orthopyroxene grains which indicates textural maturation and expulsion of interstitial liquid by compression. Most silicate crystals show grain diameters in the range between 3 and 5 mm.

Olivine in these rocks is typically anhedral to subhedral and is distributed in changing volumetric abundances throughout the intrusion. Plagioclase is typically found as laths and interstitial anhedral grains between larger grains of olivine and clinopyroxene. Clinopyroxene occurs as subhedral to anhedral grains, occasionally including smaller olivine grains. Orthopyroxene also occurs primarily as anhedral grains and often include olivine grains. This indicates a possible crystallization sequence of olivine-clinopyroxene-orthopyroxene-plagioclase.

Most of the olivine grains in Eagle and Eagle East intrusions are altered into serpentine in various intensities. Occurrences of alteration minerals like talc, chlorite and sericite and secondary minerals like calcite are also frequent. Sometimes, olivine grains are found to host small circular sulfide inclusions, which potentially represent droplets of early formed sulfide liquid.

3.1.2. Meta-sedimentary country rocks

Meta-sedimentary rocks of the Michigamme Formation surround

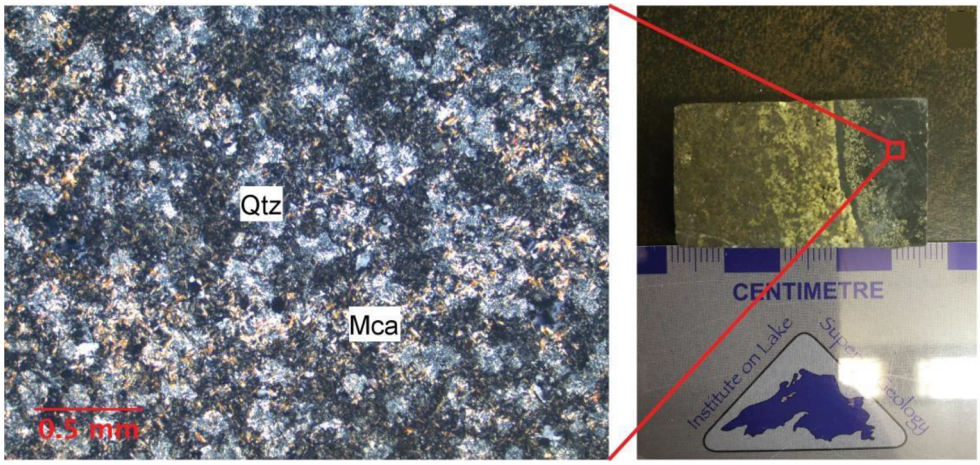

Fig. 3a. Michigamme Slate near the contract with a sulfide-mineralized zone in the intrusion. A microcrystalline groundmass of quartz, feldspar, and sericite/muscovite can be seen.

the Eagle and Eagle East intrusions. These are typically black to gray slates and have been metamorphosed to greenschist facies. Portions of the country rock immediately along the margins of the two intrusions have been contact-metamorphosed. The spatial extent of contact metamorphism around the intrusions is not uniform but thicknesses of a meter or more has been intersected by drill cores. These zones are characterized by fine-grained, interlocking, recrystallization texture. The slate unit is microcrystalline, and typically contains alternating light to dark gray bands (Fig. 3a). Occasional veins of calcite or quartz are present. Sulfide minerals sometimes seen in this rock are pyrrhotite and pyrite. The slate unit is pelite-dominated, and it is interbedded with moderate amounts of meta-graywacke. Country rocks throughout the area are associated with high amounts of graphite.

3.1.3. Archean basement rocks

Archean basement rocks under the Baraga basin consist of granites and banded gneissic rocks. Typical samples contain approximately 40% plagioclase, 30–35% quartz, and 10% feldspar. Occasional calcite veins crosscut these rocks. Pyrite and chalcopyrite also occur as euhedral to subhedral disseminated grains (Fig. 3b).

3.2. Sulfide deposits

At Eagle and Eagle East intrusions, sulfide occurrences have been classified (Ding et al., 2010) into three types: (1) disseminated sulfide, (2) semi-massive sulfide, and (3) massive sulfide. This textural classification scheme has been used in this study for its apparent simplicity and the observed zonal variations of sulfide deposits in the Eagle and Eagle East intrusions.

3.2.1. Disseminated sulfide

Disseminated sulfides contain between 3 and 15% sulfide minerals by volume, occupying the interstitial spaces between silicate minerals such as olivine and pyroxene (Fig. 3c). Such sulfide minerals are widely distributed in large sections of the peridotitic rocks. Sulfide minerals in this group form irregularly shaped, poly-mineralic blebs of pyrrhotite, pentlandite, and chalcopyrite. Pyrrhotite usually occurs either as anhedral or subhedral grains. Chalcopyrite typically occurs as intergrowths with pyrrhotite crystals. Small subhedral grains of pentlandite are often included within grains of pyrrhotite. Occasionally, pentlandite forms exsolution flame laminae within pyrrhotite crystals. The approximate grain diameter is 1 mm or less.

3.2.2. Semi-massive sulfide

Semi-massive sulfides contain 30–50% sulfide minerals and typically form interstitial net-textured arrangements with olivine, pyroxene, and plagioclase (Fig. 3d). Sulfide minerals include pyrrhotite, chalcopyrite, and pentlandite. Pyrrhotite occurs as anhedral to subhedral crystals and typically forms the base of the sulfide matrix enclosed between the silicate crystals. Chalcopyrite and pentlandite form rim-like zones around pyrrhotite grains. Chalcopyrite is also seen as cross-cutting veins within grains of pyrrhotite.

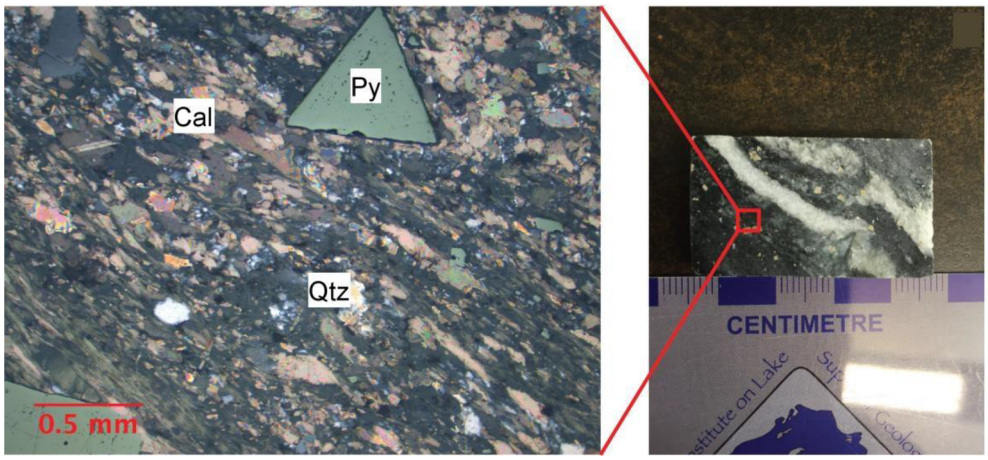

Fig. 3b. Foliated basement gneiss crosscut by calcite veins. The sample shows euhedral pyrite crystals.

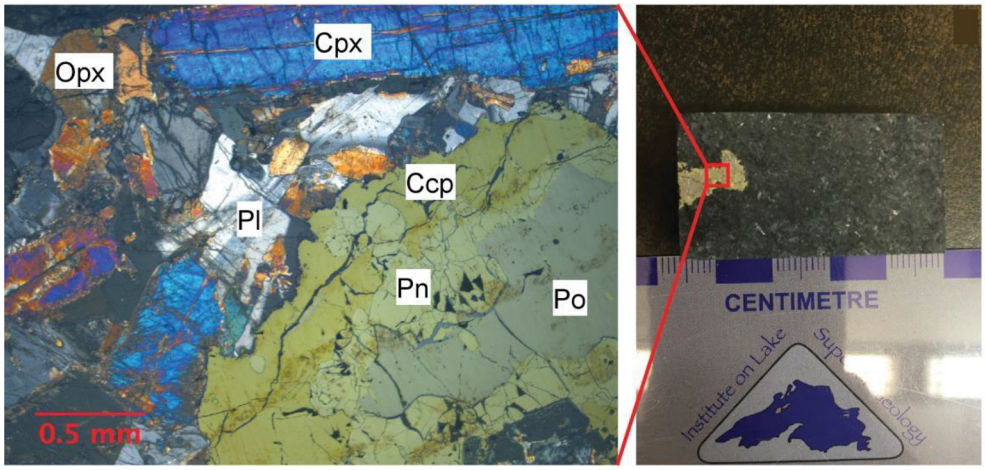

Fig. 3c. Disseminated sulfide ore in an ultramafic rock. Orthopyroxene, clinopyroxene, and plagioclase grains are seen near blebs of chalcopyrite, pentlandite, and pyrrhotite.

3.2.3. Massive sulfide

Massive sulfides contain the highest amount of sulfide minerals. These are typically composed of pyrrhotite matrix with cross-cutting veins of chalcopyrite and pentlandite (Fig. 3e). Pyrrhotite occurs as massive bands of anhedral grains, sometimes surrounding small pockets of pentlandite and chalcopyrite grains. The grain diameter of pyrrhotite crystals ranges from 500 μm to approximately 1 mm. The veins are 100 μm or less.

3.3. Sulfur isotope ratios

A total of 150 sulfide samples were analyzed for $\delta^{34}S$ values in this study: 75 from the Eagle intrusion, 34 from the Eagle East intrusion and 41 from the country and basement rocks surrounding the intrusions. $\delta^{34}S$ values collected from individual samples from portions of the Eagle intrusion are shown in Table 2 (a–d), classified with respect to the textural types. $\delta^{34}S$ values obtained from the Eagle East intrusion, arranged similarly, are shown in Table 3 (a–d). In Table 4a and b, the $\delta^{34}S$ values from sulfide mineral samples in the country and basement rocks around the Eagle and East Eagle intrusions are shown.

The sulfide minerals from the massive, semi-massive and disseminated parts of the sulfide mineral deposit and non-economic parts of the Eagle intrusion typically show $\delta^{34}S$ values ranging from 1‰ to 4‰ (Fig. 4a). There are a few samples that fall outside this range, but those occurrences are local. Most (17 out of every 20) $\delta^{34}S$ values obtained from the Eagle intrusion lie in the range between 1 and 3‰. In the Eagle East intrusion, similar values are observed and most $\delta^{34}S$ values range between 0 and 3‰ (Fig. 4b).

A very large range and spatial heterogeneity is observed in slaty and phyllitic samples from the Michigamme Formation which surround both intrusions. Sulfides from siltstone and slate taken from the surrounding country rocks around the Eagle intrusion have $\delta^{34}S$ values from 4 to 36‰ (Fig. 4a). Archean basement gneisses taken from the study area display $\delta^{34}S$ values ranging from −9 to 13‰ (Fig. 5b).

4. Discussion

4.1. Observed distributions of $\delta^{34}S$ values

In massive, semi-massive and disseminated sulfide deposits of both the Eagle and Eagle East intrusions the $\delta^{34}S$ ratio varies mostly within a tight range between 1 and 3‰ (Tables 2 and 3). However, in the metamorphosed supracrustal rocks of Michigamme Formation surrounding the intrusions, the values are significantly higher and vary over a much greater range between 5 and 36‰ (Table 4b). In the contact metamorphosed hornfelsic country rocks around the intrusion the ratio ranges between 5 and 20‰ (Table 4a). In the granite-gneissic Archean basement rocks of the Baraga basin, the ratio also varies in a wide range between −9 and 13‰ (Table 4c). In this work, the $\delta^{34}S$ values have been traced three-dimensionally along multiple directions at various

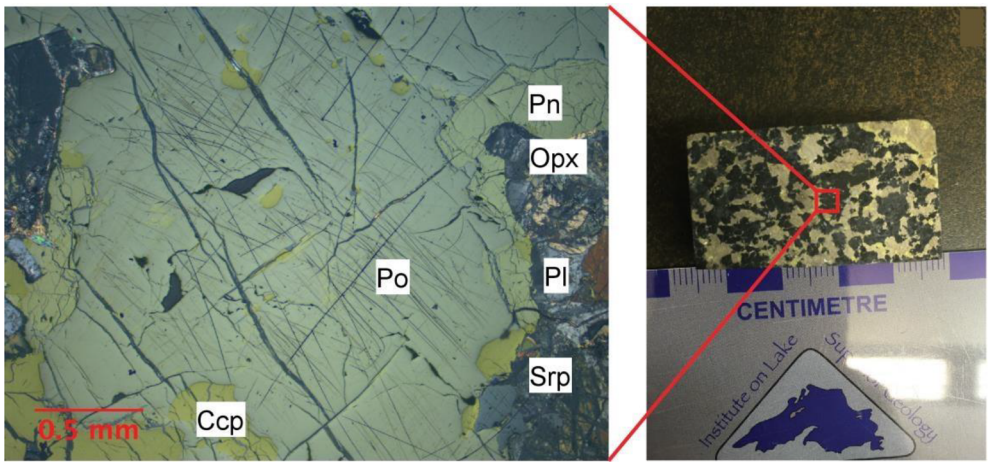

Fig. 3d. Semi-massive sulfide ore in altered ultramafic rock with orthopyroxene and plagioclase. Fine lamellae of chalcopyrite and pentlandite are hosted within pyrrhotite.

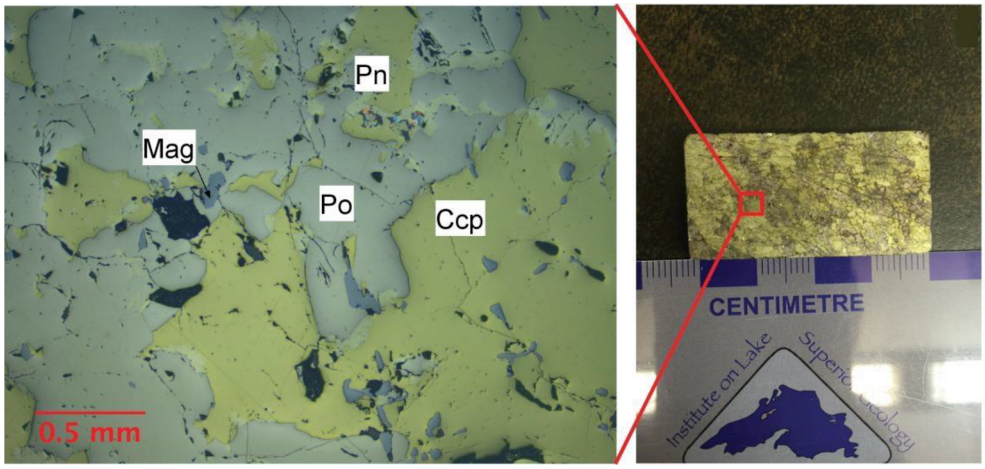

Fig. 3e. Massive sulfide ore with pyrrhotite matrix hosting chalcopyrite and pentlandite stringers. Qtz = quartz; Mca = mica; Calc = calcite; Cpx = clinopyroxene; Opx = orthopyroxene; Pl = plagioclase feldspar; Po = pyrrhotite; Ccp = chalcopyrite; Pn = pentlandite; Srp = serpentine; Mag = Magnetite.

depths using drill core samples as shown in Figs. 6 and 7. The drill cores can be seen to cut across sulfide ore-horizons within the intrusions, the outlines of which have been defined by the three observed textural types: massive, semi-massive and disseminated. There is no significant relationship between the $\delta^{34}S$ values of sulfide minerals within the intrusion, with (1) types of texture; (2) locations of samples, i.e., in the interior of the intrusion or along the peripheral areas close to the wall rocks or (3) mineral (pyrrhotite, chalcopyrite, and pentlandite).

It has been established by many workers that the assimilation of S-rich crustal rocks is very important for sulfide saturation of a mantle-derived magma (Ripley and Li, 2003; Arndt et al., 2005; Barnes and Lightfoot, 2005; Keays and Lightfoot, 2010; Ripley and Li, 2013). For the Eagle deposit, Ding et al. (2011) calculated that fractional crystallization of the parental magma, with an initial content of mantle-derived S would not be enough to induce sulfide saturation. Thus, the addition of external S from crustal rocks must have occurred. The degree of assimilation of S from external sources can be calculated by using S-isotope systematics (Ripley and Li, 2003; Ripley and Li, 2013). The relative homogeneity of $\delta^{34}S$ values within the sulfide portions of the intrusion and the stark contrast of such values in sulfide minerals from surrounding rocks might seem anomalous with the premise that sulfide saturation in the magma was caused by the incorporation of S from the crustal rocks during uplift. Moreover, the overall volumes of sulfide deposits in the intrusions when compared with the observed content of sulfur in the surrounding rocks, it is obvious that most of the sulfide in the magma was formed by cumulative addition of sulfur from the wallrocks of the conduit at many levels. New batches of sulfide liquid must have been added by continued assimilation and devolatilization of wallrocks at progressively shallower levels during magmatic ascent. Some of the sulfide liquid could also have migrated downward by gravity from upper levels, at the waning stages of magmatism (Hughes et al., 2016).

For a mantle-derived sulfide-undersaturated magma, sulfide saturation must have been induced by assimilation of crustal sulfur. Sulfur in pristine mantle-derived magma is known to possess $\delta^{34}S$ values in the narrow range of 0 ± 2‰ (Ripley and Li, 2003; Ripley and Li, 2013). But, the final $\delta^{34}S$ values measured from sulfide minerals within the intrusion, represent a weighted sum of $\delta^{34}S$ values from mantle-derived sulfur and the sulfur introduced by the assimilation of crustal rocks.

The contribution of sulfur from the crustal rocks could be substantial. For instance, in the Cu-PGE-Au sulfide mineralization in the Paleogene macrodikes of the Kangerlussuaq region in Greenland, the $\delta^{34}S$ values range between −10.4 and −25.7‰ (Holwell et al., 2012). This significant departure of $\delta^{34}S$ values from the mantle range was consistent with the input of sulfur from the local marine sedimentary rocks of the Kangerlussuaq Basin. In the Platreef Ni-Cu-PGE deposit in the Bushveld Complex of South Africa, variations in sulfur isotope ratios at different levels and locations could be explained by $\delta^{34}S$ signatures representative of magmatic sulfur as well as country rock sulfur (Holwell et al., 2007). In the early formed sulfide droplets, the mantle range of $\delta^{34}S$ values: 0 ± 2‰ was detected. However, later sulfides above calc-silicate floor-rocks, show a mean $\delta^{34}S$ value of 4.4‰ which indicated sulfur input from anhydrite-bearing horizons of the Malmani Dolomite with high $\delta^{34}S$ signatures. It was interpreted that the Archean basement rocks with negative $\delta^{34}S$ values did not contribute much sulfur to the Platreef deposit.

Lesher (2017) argued that S-isotope values similar to mantle may not necessarily indicate mantle derivation but could also imply sulfur source rocks where the S-isotopes had not fractionated from mantle values. The deepest known crustal rocks around Eagle and Eagle East intrusions are the Archean granite-greenstone basement rocks of the Baraga basin. The $\delta^{34}S$ values in basement rock have been found to show high degrees of departure from the known mantle-range (Table 4c). So, it is highly likely that the source rocks for the magma were indeed in the mantle and the magma had been contaminated significantly by assimilations of crustal rocks. It is also possible that large degrees of assimilation of the granitic basement rock might have partially induced sulfide saturation (Irvine, 1975; Li and Naldrett, 2000; Lightfoot and Hawkesworth, 1997; Seat et al., 2009).

$\Delta^{33}S$ values of sulfide minerals have also been used in many instances to characterize the sources of sulfur in magmatic systems (Penniston-Dorland, 2008; Sharman et al., 2013; Ripley and Li, 2017). Ding et al. (2012) observed variations in the $\Delta^{33}S$ values of sulfide minerals hosted in the Eagle intrusion and reported that $\Delta^{33}S$ values within the semi-massive sulfide unit vary between −0.86 and 0.86‰, whereas the massive and disseminated sulfides showed values in the range from −0.10 and 0.09‰. The small range in $\Delta^{33}S$ values in the massive and disseminated sulfides indicates that the S in these minerals was derived from Proterozoic source rocks, while the massive and disseminated sulfides with larger variability in $\Delta^{33}S$ values were derived from Archean source rocks. This suggests two episodes of sulfide emplacement, one from the Archean basement rocks and another from the Paleozoic supracrustals. More recently, Benson et al. (2018) argued that $\Delta^{33}S$ values from the Eagle East deposit range between −0.07 and 0.05‰ and these values do not indicate significant involvement of sulfur from Archean rocks. A study of the spatial distribution of $\Delta^{33}S$ values in sulfide minerals within the intrusions and in the surrounding rocks is beyond the scope of this study but we have traced the point by point variation of $\delta^{34}S$ signatures within the intrusion, in relation to

Table 2
S-isotope ratios from portions of the Eagle intrusion.

a. Disseminated sulfide

Drill Core	Depth (m)	$\delta^{34}S$ (‰)
EAUG0011	32.75	1.2
EAUG0012	30.72	2.0
EAUG0012	77.01	1.2
04EA054	27.7	2.6
04EA073	153.02	0.7
EUGX0007	65.94	3.1
12EA273A	329.22	1.6

b. Semi-massive sulfide

Drill Core	Depth (m)	$\delta^{34}S$ (‰)
EAUG0011	44.55	3.8
EAUG0012	48.82	−1.5
04EA083	30.9	1.3
04EA083	100.22	2.3
04EA054	32.45	1.7
04EA054	82.1	2.1
04EA054	98.9	2.1
04EA054	154.68	2.7
12EA269	346.8	−5.8
12EA269	348.15	−1.0
12EA269	382.37	−0.6
04EA073	165.5	1.9
04EA073	215.1	2.2
EUGX0007	42.5	−0.8
12EA273A	289.35	2.1
12EA273A	317.17	−3.2
12EA273A	321.65	3.0
12EA273A	331.04	1.7
EAUG0300	0.81	2.5
EAUG0300	9.52	2.9
EAUG0300	18.13	2.9
EAUG0300	24.39	3.0
EAUG0300	37.53	3.1
EAUG0300	43.95	3.1
EAUG0300	44.15	2.9
EAUG0300	55.93	3.0
EAUG0300	58.47	3.1
EAUG0300	60.39	3.1
EAUG0300	66.24	3.1
EAUG0300	83.43	2.7
EAUG0300	84.53	3.1
EAUG0301	2.63	2.7
EAUG0301	16.3	3.0
EAUG0301	19.66	3.0
EAUG0301	26.5	3.0
EAUG0301	40.96	3.0
EAUG0301	49.14	2.6
EAUG0301	57.89	3.8
EAUG0301	60.17	3.1
EAUG0301	70.31	3.0
EAUG0301	78.17	2.9

c. Massive sulfide

Drill Core	Depth (m)	$\delta^{34}S$ (‰)
EAUG0011	48.02	−3.8
EAUG0011	60.37	3.9
EAUG0011	74.9	1.8
04EA083	181.01	2.4
04EA054	230.8	2.5
04EA054	235.87	1.6
04EA054	247.72	2.6
04EA054	286.97	−0.8
12EA269	347.5	1.5
12EA269	351.51	1.3
04EA073	177.15	3.4
04EA073	244.57	2.6
EUGX0007	69.69	1.9
EUGX0007	72.31	2.3

Table 2 (*continued*)

c. Massive sulfide

Drill Core	Depth (m)	$\delta^{34}S$ (‰)
12EA273A	312.8	1.7
12EA273A	314.98	2.9
12EA273A	318.67	1.1
12EA273A	326.17	−5.2
12EA273A	335.39	1.7
03EA032	298.59	3.0
03EA032	306.57	−0.2

d. Peridotitic host rock

Drill Core	Depth (m)	$\delta^{34}S$ (‰)
04EA083	25.32	1.2
04EA073	129.04	3.7
04EA073	221.76	2.8
12EA273A	274.05	2.2
03EA032	295	3.7
03EA032	328.18	−1.8

observed values in the country and basement rocks. From the intrinsic association of the three sulfide domains within the intrusion and the interfingering nature of their occurrences, as revealed in drill core studies and shown in Figs. 6 and 7, identification of two distinct and specific magmatic pulses within the intrusion, based on sulfide textures seems very challenging. We propose incremental addition of small batches of sulfide liquid from the country rocks and homogenous mixing of immiscible sulfide liquids for both Eagle and Eagle East intrusions.

4.2. Dynamic conduit system model

In both Eagle and Eagle East intrusions, large volumes of sulfide deposits, relative to the overall sizes of the intrusions clearly indicate substantial contribution of external sulfur in the magmatic system (Lesher et al., 1984; Li and Ripley, 2005; Keays and Lightfoot, 2010; Ripley and Li, 2013). The near-conical shapes of the intrusions, and narrow pipe-like feeder channels underneath, as delineated by exploratory drill-core studies, reveal structures which can be regarded as magmatic conduit-systems (Fig. 2). From the 1.1 Ga age of the Eagle intrusion (Ding et al., 2010), these conduits could be interpreted as feeder systems which led to surficial volcanism during the Midcontinent Rift event. The Tamarack deposit in Minnesota has also been identified as a similar conduit-type magmatic sulfide deposit associated with the Midcontinent Rift (Taranovic et al., 2016)

The observed high grades of Ni (~6.5% in the massive sulfide ore) and Cu (~3.8% in massive sulfide ore) at the Eagle and Eagle East deposits can be explained by chemical interactions of small batches of immiscible sulfide liquids with large quantities of mantle-derived magma, with high silicate liquid to sulfide liquid ratio, also called the R-factor (Campbell and Naldrett, 1979; Kerr and Leitch, 2005; Lambert et al., 1998). This process has been reported for world-class magmatic sulfide deposits such as Norilsk (Brügman et al., 1993; Naldrett and Lightfoot, 1993; Naldrett, 2004; Lightfoot and Keays, 2005). Large volumes of magma required for the dynamic upgrade of the segregated sulfide liquid is consistent with the assertion that these conduits acted as feeder channels for volcanic eruptions on the surface. Very high sulfide ore-grade: 8.36% Ni, 14.08% Cu and 107.17 ppm Pt + Pd (Naldrett, 2004) at Norilsk is explained by the enormous magmatism along near-vertical conduits associated with the Permo-Triassic Siberian Trap volcanics. Repeated magmatic upheavals progressively upgraded the content of chalcophile elements in the sulfide liquid trapped along the magmatic flow path (Brügman et al., 1993; Naldrett et al., 1995). However, the distribution of $\delta^{34}S$ values is not uniform at

Table 3
S-isotope ratios from the mineralized zones in the Eagle East intrusion.

a. Disseminated sulfide

Drill Core	Depth (m)	$\delta^{34}S$ (‰)
08EA222D	308.0	0.6
EUGX0035	247.5	3.2
EUGX0040	372.6	−0.8
EUGX0040	390.5	0.7
14EA331H	1142.0	1.2
14EA331I	1139.8	5.3
14EA331I	1141.4	3.8
14EA331I	1143.2	2.8

b. Semi-massive sulfide

Drill Core	Depth (m)	$\delta^{34}S$ (‰)
08EA222D	256.9	−4.0
EUGX0040	392.2	1.4
14EA331H	1148.6	2.3
14EA331H	1150.2	2.3
14EA331I	1145.4	−2.1
14EA331I	1166.0	1.1
14EA331I	1167.8	2.9

c. Massive sulfide

Drill Core	Depth (m)	$\delta^{34}S$ (‰)
EUGX0035	252.6	0.3
EUGX0035	253.1	1.3
EUGX0035	253.4	2.6
14EA331G	1162.7	0.4
14EA331G	1165.3	1.7
14EA331G	1167.5	5.0
14EA331H	1153.4	−0.8
14EA331H	1156.2	0.8
14EA331H	1161.4	0.9
14EA331H	1165.2	1.5
14EA331H	1165.6	1.3
14EA331I	1145.7	3.0
14EA331I	1146.0	−0.2
14EA331I	1153.7	1.3
14EA331I	1159.6	1.1
14EA331I	1168.9	0.6
14EA331I	1170.6	1.5

d. Peridotitic host rock

Drill Core	Depth (m)	$\delta^{34}S$ (‰)
14EA331G	1161.6	0.1
14EA331H	1140.6	2.3

Table 4
S-isotope ratios in the country-rocks and basement rocks around Eagle and Eagle East intrusions.

a. Contact-metamorphosed country rocks

Drill Core	Depth (m)	Rock Type	$\delta^{34}S$ (‰)
04EA083	197.7	Hornfels	5.1
12EA269	382.7	Hornfels	7.6
12EA273A	343.9	Hornfels	9.6
03EA032	283.5	Hornfels	8.8
08EA222D	311.9	Hornfels	19.5
14EA331G	1167.8	Hornfels	5.9
14EA331H	1166.4	Hornfels	17.9

b. Paleoproterozoic country rocks

Drill Core	Depth (m)	Rock Type	$\delta^{34}S$ (‰)
12EA269	339.2	Slate	6.8
DL-1	415.0	Slate	5.8
DL-1	530.5	Slate	9.6
DL-3b	294.9	Slate	19.3
DL-4	471.5	Slate	7.6
EUGX0040	566.7	Slate	7.7
14EA331	1173.1	Slate	19.7
17EA364	1081.1	Slate	33.7
17EA364	1085.5	Slate	32.6
17EA364	1089.7	Slate	32.7
17EA364	1096.1	Slate	30.9
17EA364	1100.8	Slate	29.7
17EA364	1071.9	Slate	33.4
17EA364	1000.0	Slate	35.4
17EA60D	1323.2	Slate	4.0
17EA60D	1330.0	Slate	5.1
17EA60D	1339.6	Slate	6.7
17EA60D	1352.3	Slate	5.7
17EA60D	1367.6	Slate	5.3
17EA60D	1384.5	Carbonate rock/vein	11.7
17EA60D	1395.4	Carbonate rock/vein	5.8
17EA60D	1395.5	Carbonate rock/vein	5.3
DL-7	177.5	Carbonate rock/vein	13.4
08EA222A	700.3	Meta-graywacke	7.7
08EA222A	709.0	Meta-graywacke	5.9

c. Archean basement rocks

Drill Core	Depth (m)	Rock Type	$\delta^{34}S$ (‰)
12EA296A	1858.1	Banded gneiss	7.8
12EA296A	1903.1	Gneiss with graphite	2.6
12EA296A	1916.0	Banded gneiss	−0.2
08EA183	1661.2	Granite-gneiss	2.5
08EA184	1681.7	Granite-gneiss	−7.4
08EA184	1689.7	Granite-gneiss	−9.4
17EA360D	1417.3	Calcite vein in granite-gneiss	12.6
17EA360D	1604.0	Granite-gneiss	1.2
17EA360D	1637.5	Granite-gneiss	3.4

Norilsk. Works of Gorbachev and Grinenko (1973), Grinenko (1985) and Ripley et al. (2003) have demonstrated that the $\delta^{34}S$ ratios in sulfide minerals associated with the Norilsk deposit vary within a wide range. In intrusions with S-content up to 0.4 wt%, the $\delta^{34}S$ values range between 5.5 and 8.4‰, while sills with S-content less than 0.1 wt% show values ranging between −7 and 16‰. Values close to that of mantle-derived sulfur represent S-poor parts of the intrusion, but S-rich occurrences show greatest deviations from the mantle-range. This was interpreted as a clear indication that assimilation of crustal sulfur was associated with the chalcophilic metal enrichment in the Norilsk sulfide deposit (Ripley and Li, 2003; Li et al., 2003). The principal sources of crustal sulfur were layered evaporite deposits with $\delta^{34}S$ values of about 20‰ (Gorbachev and Grinenko, 1973).

At the conduit-type Ni-Cu sulfide deposit of Voisey's Bay in Labrador Province, Canada, the observed systematic variations of $\delta^{34}S$ signatures have been explained with respect to 20–30% assimilation of a sulfide-bearing partial melt from a Proterozoic country rock, the Tasiuyak paragneiss (Ripley et al., 1999). $\delta^{34}S$ values of the Tasiuyak paragneiss range from −0.9 to −17.0‰. In the sulfide mineralized parts of the Voisey's Bay intrusion, $\delta^{34}S$ values show specific ranges based on the rock type and calculated degrees of contamination. In the Reid Brook Zone, surrounded by the Tasiuyak paragneiss, the $\delta^{34}S$ values are consistently negative, between −4.1 and −1.1‰, while in the Eastern Deeps Zone, away from the paragneiss, the values range between −0.5 and 1.8‰ (Ripley et al., 1999).

These two deposits demonstrate two different scenarios. In the case of Norilsk, the $\delta^{34}S$ ratios in the sulfide deposits are highly variable but their values could be modeled using different degrees of contamination from isotopically uniform evaporite beds. In the case of Voisey's Bay, the $\delta^{34}S$ ratios are variable on a modest degree with contaminations from an isotopically diverse Tasiuyak paragneiss country rock. The Eagle sulfide deposit represents a third scenario, in which the $\delta^{34}S$ values in the sulfide deposit fall within a very small range but, values in

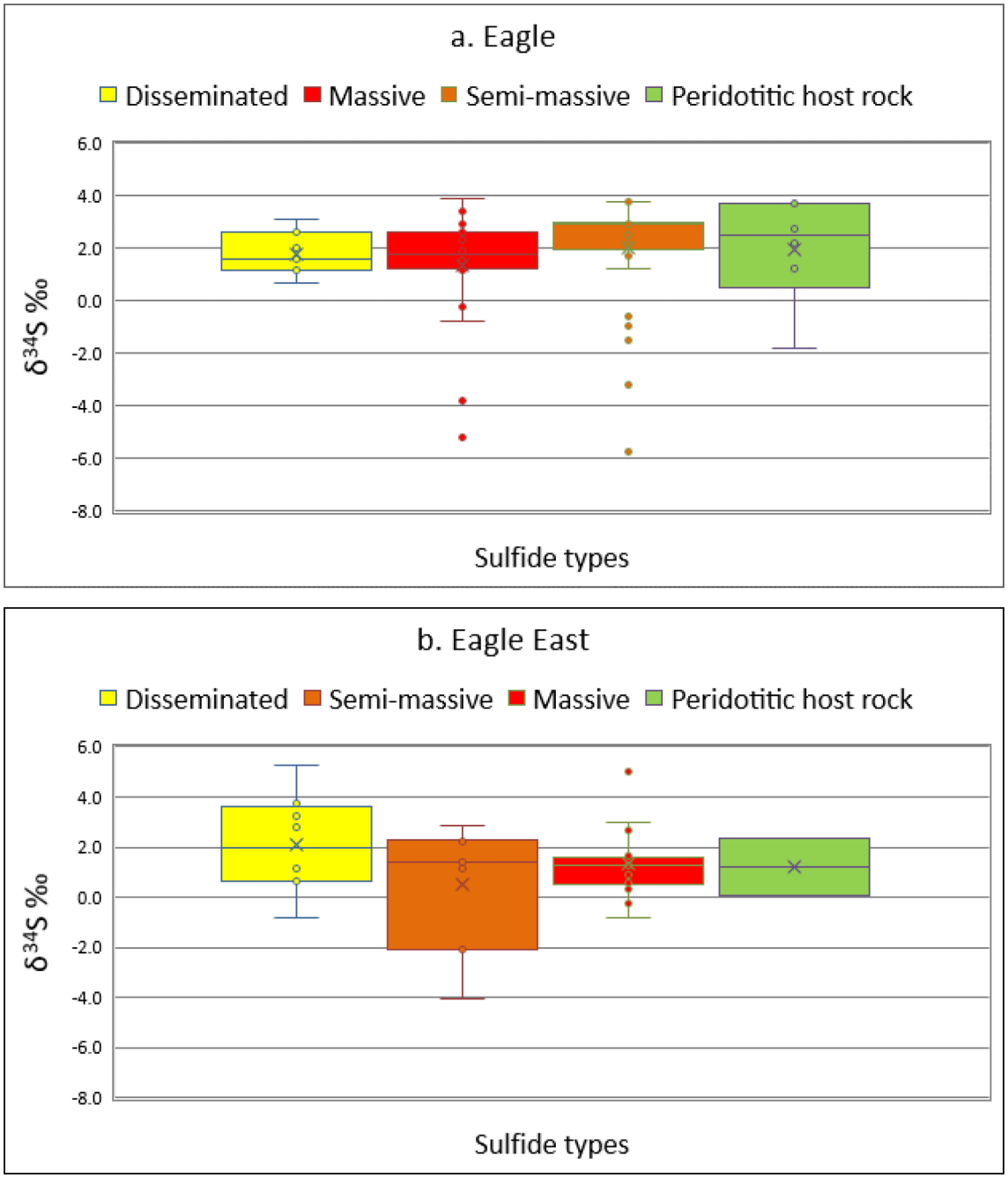

Fig. 4. Measured ranges of $\delta^{34}S$ values from the different types of sulfide occurrences in (a) Eagle and (b) Eagle East intrusions.

the adjoining country rocks are widely and inconsistently variable. Using R-factor values between 200 and 350, Ripley and Li (2013) calculated that the interaction of about 2 km^3 of a mantle-derived picritic magma with an immiscible sulfide liquid along the conduit system is consistent with the size and the ore grade observed at the Eagle sulfide deposit. This estimate seems very reasonable for the reported volumes of magmatism associated with the early development of the Mid-continent Rift system (Stein et al., 2018).

The observed $\delta^{34}S$ values in the Eagle sulfide deposit and the country rocks can be modeled using different degrees of mixing between mantle-derived magma with country rocks of known $\delta^{34}S$ values. In our calculation, based on the estimates of S in a picritic magma (Ripley and Li, 2013) we use a magma with 1000 ppm of S with a $\delta^{34}S$ value of 0‰. This magma assimilates crustal rocks with an average 1% S and an average $\delta^{34}S$ value of 7.7‰, which is the median value from the Michigamme Formation. With an R-factor of 200 and assuming complete mixing, the $\delta^{34}S$ value of the sulfide liquid will be 0.4‰. It can be calculated that with widely variable $\delta^{34}S$ values in the country rocks, higher values of R-factor will bring the $\delta^{34}S$ of the mixed sulfide liquid closer to the mantle range of 0 ± 2‰.

The average $\delta^{34}S$ of 2.5‰ in the granitic basement rock indicates that a uniform assimilation of sulfides from this source, could keep the magmatic $\delta^{34}S$ value close to the mantle range. However, the incorporation of sulfur from the shallower Paleoproterozoic country rocks with a much wider $\delta^{34}S$ range could locally distort $\delta^{34}S$ values in shallower parts of the intrusion. So, there must have been an inherent process of homogenization of $\delta^{34}S$ values all through the magmatic flow-path, particularly near the surface.

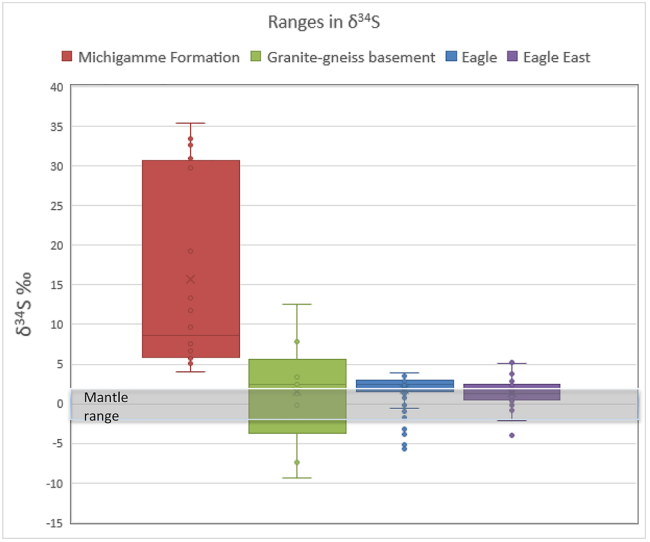

Fig. 5. Observed ranges of $\delta^{34}S$ values from Eagle and Eagle East intrusions and the potential sulfur source rocks of Michigamme Formation and basement granite-gneiss. Mantle range is indicated by the gray box.

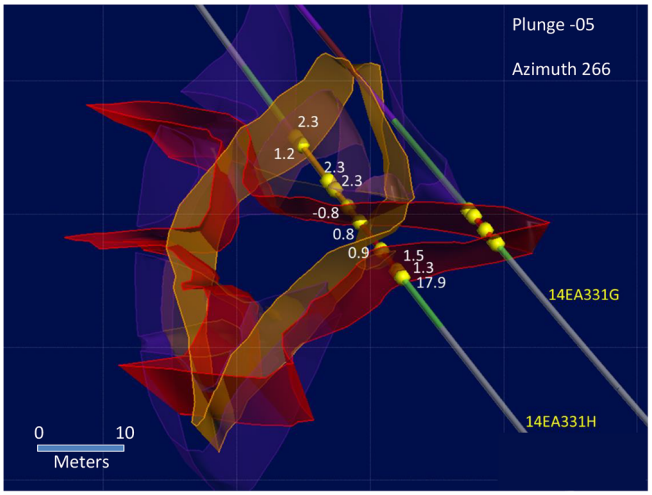

Fig. 6. Distributions of $\delta^{34}S$ values obtained from sulfide minerals in various portions of the Eagle intrusion and country rocks traced along drill cores. The drill core numbers are given in each figure. Colored shells indicate outer margins of different ore types. Red is massive, orange is semi-massive, and purple is disseminated. Blue represents the country rocks. The colored sections of the drill-cores indicate the sulfide ore type in that portion of the core. (Prepared with assistance from Espree Essig, Samantha Kleich and Bob Mahin).

4.3. Possible mechanisms for homogenization of $\delta^{34}S$ values

In a dynamic flow-through magma conduit at Eagle, after sulfide saturation was achieved at depth, a mixture of magma, silicate crystals and droplets of the immiscible sulfide liquid must have moved upward (Ding et al., 2010). Any additional sulfur introduced by direct assimilation of country rocks or by the incorporation of S-rich vapor phase, could not remain dissolved in the magma but would appear as new immiscible sulfide droplets. Such new sulfide droplets carry S-isotope ratios representative of the S-minerals in the country rocks. It is intuitive that these new sulfide droplets appear at the fringes of the magma column near the contact with country rocks.

Wallrocks are fragmented and entrained into the flowing magma along the edges of the conduit by thermal and mechanical erosion (Figs. 8 and 9). These xenoliths are pulled into the interior of the conduit by kinetic turbulence and get mechanically disintegrated and

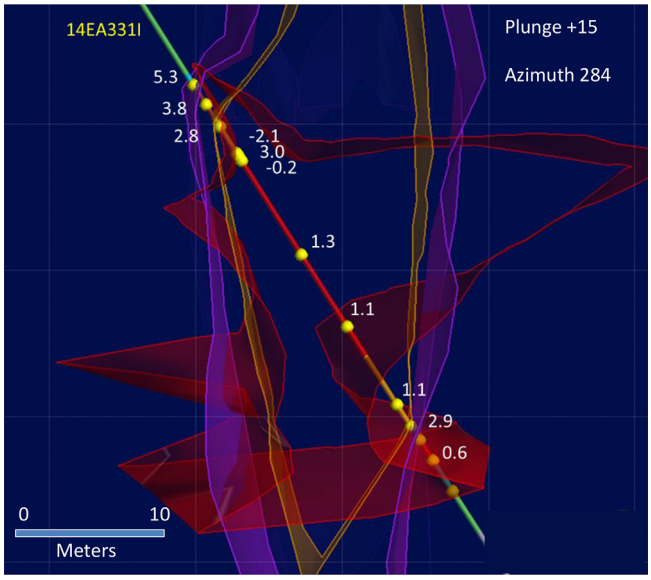

Fig. 6. (*continued*)

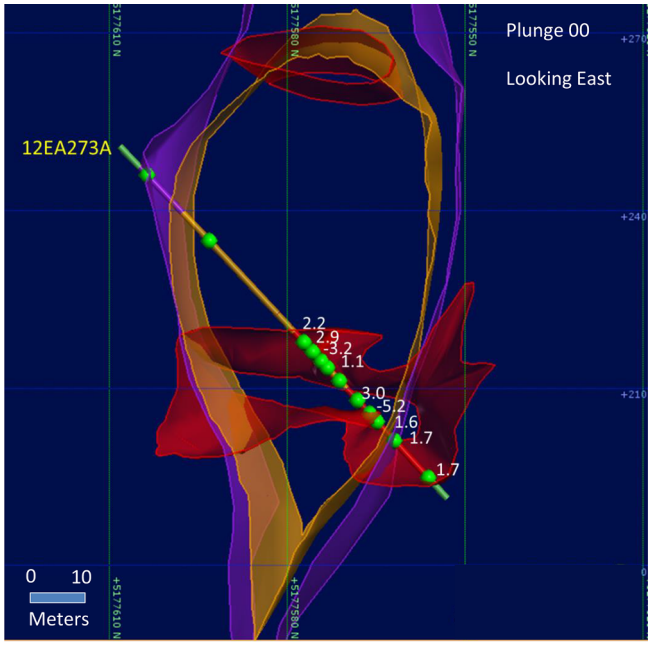

Fig. 6. (*continued*)

subsequently melted in the magma (McLeod and Sparks, 1998). The silicate portions of these fragments get dissolved into the magma, but if the magma is sulfide-saturated, the sulfide portions of the fragments get dispersed as tiny immiscible droplets (Samalens et al., 2017). Several workers such as Barnes and Lightfoot (2005), Keays and Lightfoot (2010), Ripley and Li (2013), Lesher (2017), and Barnes and Robertson (2019) have concluded that the mechanism of "xenomelts" is a powerful mechanism of transfer of crustal sulfur into magmatic systems. Xenoliths of country rocks have not been found in the Eagle intrusions, but the observed homogeneity in $\delta^{34}S$ values from Eagle intrusions, clearly indicates that regardless of the mechanism of sulfur incorporation from crustal rocks, there must have been a process to account for the mixing of the sulfide liquids in the conduit. The incorporation of crustal sulfur into the magma at shallow levels must have occurred by the transfer of country rock xenoliths, but the newly formed sulfide droplets must have been homogeneously intermixed with the already existing sulfide liquid in the system.

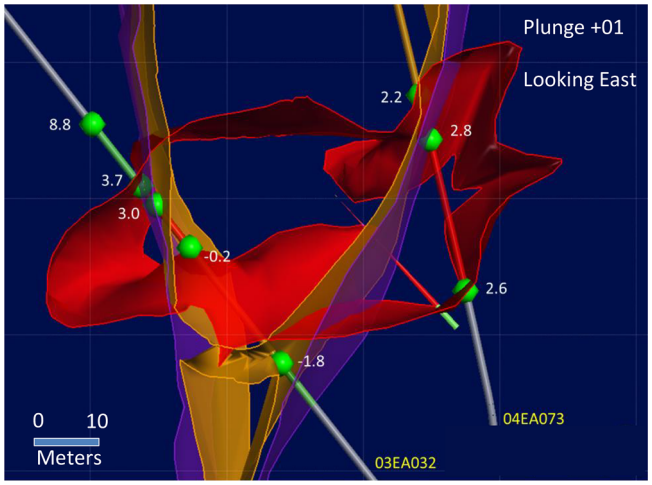

Fig. 6. (*continued*)

Based on studies of velocity profiles of magmas in near-vertical conduits (Komar, 1976; Correa-Gomes et al., 2001) it can be argued that in a hypothetical cylindrical magma column inside a dynamic conduit, the highest flow rate is at the central axis, and the flow-rate gradually decreases from the center towards the edges where the magma is in direct contact with the country rocks. According to the flowage differentiation mechanism (Bhattacharji and Smith, 1964; Ross, 1986), the central axis has the highest concentration of crystals. New crystals preferentially form along the lower temperature zone at the edges of the magma column with a higher abundance of nucleation sites. The new crystals are pulled to the central axis by the rising magmatic pulse. It is possible that the internal friction and attrition of the moving crystals caused by the turbulence of the rising magma column could churn the mass of immiscible sulfide liquid during travel along the conduit (Robertson et al., 2015). Since silicate crystals and sulfide liquid droplets move at different velocities owing to density differences, the process of separating and re-mixing of the sulfide blobs by moving crystals in a flowing magma column could be very effective. There is no gradation of $\delta^{34}S$ values from the internal part of the intrusion to the periphery. This implies near uniform mixing and homogenization of all immiscible sulfides in the system, whether along the edges of the conduit or in the interior.

Gaetani and Grove (1999) and Mungall and Su (2005) suggested that when sulfide liquid droplets form as a discrete immiscible phase in a silicate magma, these tend not to wet the surfaces of silicate or oxide minerals and thus, do not flow in cohesion with such minerals in a dynamic magma conduit. So, the sulfide liquid droplets preferentially lag behind and intermix in a magma flow column. Lesher and Groves (1986) explained that upon sulfide saturation, the suspended sulfide droplets break-up by shearing stress near the flow margins or by internal turbulence within the magma column. Droplet coalescence is possible only in relatively static environments where the droplets are in mutual contact for prolonged periods of time and are not separated by dynamic forces such as flow turbulence and crystal transport. Robertson et al. (2016) argued that droplet break-up is more predominant in dynamic magma conduit systems. The widespread dispersal of fine sulfide droplets in the magma could expose larger surface areas of the sulfide liquid to the silicate magma, than large coalesced sulfide liquid aggregates. This could lead greater interaction of the sulfide liquid with the metal-enriched silicate magma and thereby cause greater acquisition of Cu, Ni, PGE from the magma. The observed high ore-grade for Ni and Cu at Eagle is consistent with this argument.

Considering the notion that small sulfide liquid droplets do not coalesce in a dynamic environment, the isotopic homogeneity observed in all textural and spatial domains of the Eagle deposits deserves special attention. Every sulfide "xenomelt" droplet from the entrained xenolith from the country rocks, upon melting, must have released sulfide droplets which carry the $\delta^{34}S$ signature while in the country rock (Fig. 9). This isotopic signature must be preserved in the sulfide droplets in miniature closed systems, because the immiscible droplets do not coalesce. This would lead to a wide diversity of $\delta^{34}S$ values in the sulfide minerals which were eventually crystallized from the sulfide liquids, unless there was a mechanism of late coalescence of the droplets. The degree by which new sulfur is added to the magma from crustal sources relative to the sulfur already in the melt, is a determinative factor for the deviation of $\delta^{34}S$ values from the known mantle values. As has been reported in this study, despite wide variabilities of $\delta^{34}S$ values in the crustal sources, the observed $\delta^{34}S$ values in the intrusion are near the mantle range of 0 ± 2‰. This implies a much larger mantle- or mantle-like contribution of S in the ore forming process (Ripley et al., 2005; Thakurta et al., 2008). Assuming sulfur-assimilation from a crustal source with an average $\delta^{34}S$ of 7.7‰, as seen in the rocks of Michigamme Formation, it can be calculated that at least 70% of the sulfur in the mineral deposit was derived from a sulfur source representative of the mantle.

The Eagle and Eagle East deposits were both formed in funnel-like magma conduits (Fig. 2). Ding et al. (2010) postulated that, continued crystallization of olivine and pyroxene changed the geometry of the magma conduit of the Eagle intrusion. The funnel-like shape might indicate changing magma velocity upon entering a wide chamber,

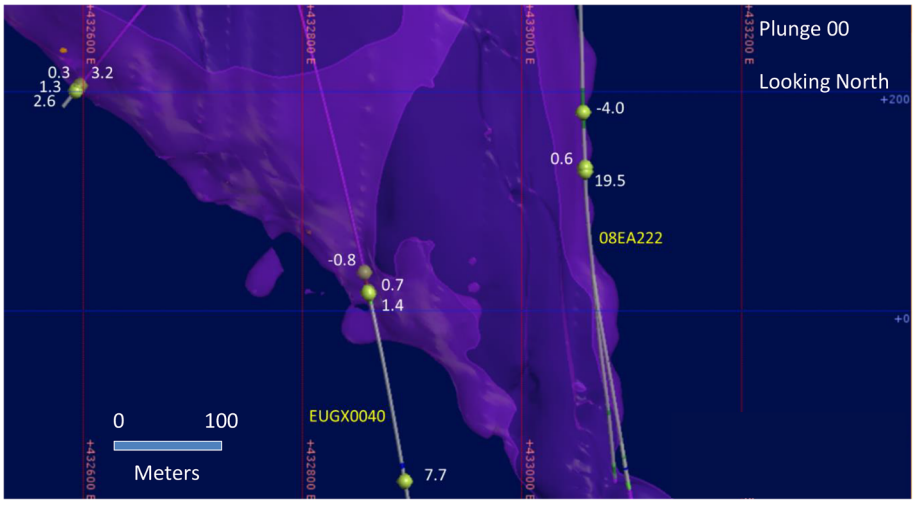

Fig. 7. Distributions of $\delta^{34}S$ values obtained from sulfide minerals in various portions of the Eagle East intrusion traced along drill cores.

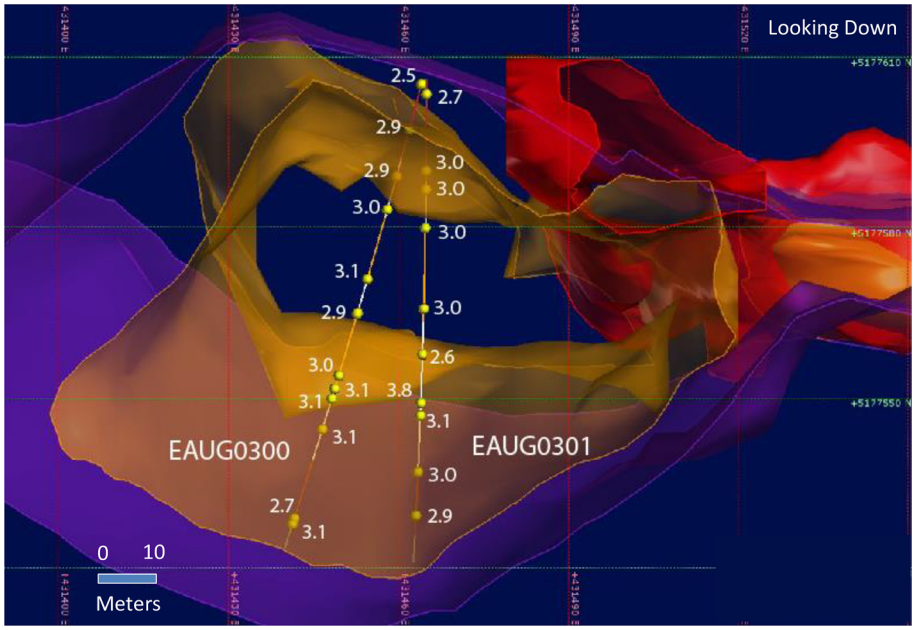

Fig. 7. (*continued*)

immediately after passing through a "bottle-neck" in the conduit. In the Eagle East intrusion the sulfide ore is found at the conduit immediately underneath a wide conical chamber (Fig. 2). This could be attributed to changing velocity of the magma caused by changes in the conduit diameter.

However, the dynamic uprise of enormous quantities of magma through the conduit must have eventually come to a halt at the waning stages of magmatism in the region. Barnes et al. (2016) and Hughes et al. (2016) proposed a mechanism by which the sulfide liquid droplets already entrained in the magma, owing to higher density, could sink back through the conduit at the end of magmatic uplift. This process of sulfide "withdrawal" in response to gravity, could be very effective in near-vertical or steeply inclined magma conduits. The slow downward movement could allow the mixing and coalescence of sulfide droplets and this could lead to the ultimate accumulation of large quantities of sulfide liquid in a structural down warp, which upon cooling, could potentially form a sulfide ore body. This model also raises the possibility that, some of the sulfide liquid could have formed by incorporation of sulfur from country rocks at levels that are much higher than the observed level of the deposit. Some of that could even be at levels which have been removed by erosion or are no longer exposed. Similar processes of late remobilization of an initial sulfide accumulation by gravitational readjustment and structural displacements have also been proposed by workers such as Naldrett (1999), Lightfoot et al. (2012), Lightfoot and Evans-Lamswood (2015) for deposits such as Voisey's Bay and Norilsk.

Another mechanism to explain the aggregation of the sulfide liquid could be the formation of a "sludge" of partially molten sulfur-rich fragments derived from the country rock and the subsequent downward percolation of the sulfide liquid from these fragments to form ore bodies as has been proposed by Barnes et al. (2017) to explain the sulfide matrix ore breccias in the Voisey's Bay sulfide deposit.

The sulfide deposits at Eagle and Eagle East deposits at the bottom of large conical chambers could indicate gravitational displacement along the steep conduit walls and subsequent accumulation of sulfide liquid as explained by Hughes et al. (2016) for the mafic-ultramafic plugs in the Isle of Rum, Scotland. This mechanism could also cause the mixing and accumulation of large quantities of entrained droplets of sulfide liquid by slow gravitational displacement and this can explain the observed homogeneity of the $\delta^{34}S$ signatures in the Eagle and Eagle East deposits. The substantial occurrence of disseminated sulfide minerals in the large conical chamber of the Eagle East intrusion just above the economic sulfide deposit is consistent with this mechanism.

5. Conclusion

1. The $\delta^{34}S$ ratios obtained from sulfide minerals within the magmatic sulfide deposits associated with the Mesoproterozoic Eagle and Eagle East intrusions mostly cluster within a tight range between 1 and 3‰ (V-CDT). The observed values do not show any relationship with the type of host rock, ore texture, type of the sulfide mineral or location of the sulfide sample in the 3D geometry of the intrusions.
2. The $\delta^{34}S$ ratios obtained from sulfide minerals in the surrounding metamorphosed Paleoproterozoic country rocks of Michigamme Formation and from the Neoarchean granite-gneiss basement rocks of the region show very wide ranges. The former shows a range between 4 and 36‰ and the latter lies in the range between −9 and 13‰.
3. The small range of $\delta^{34}S$ values within the intrusion, despite wide variabilities noticed in the surrounding rocks, has been explained by a mechanism involving homogeneous mixing of the immiscible sulfide liquid in the magma during movement along a dynamic crustal conduit.
4. Even though most of the sulfur in the magma was transported from the mantle or from a mantle-like sulfur reservoir at depth, the external sulfur added to the system from crustal levels with distinct $\delta^{34}S$ signatures was able to mix uniformly, such that final $\delta^{34}S$ of the sulfide mixture was a weighted average of $\delta^{34}S$ values from all the sources of sulfur.
5. The homogeneous mixing of the immiscible sulfide liquid was achieved by an internal turbulence caused by mutual interactions between crystals, entrained wall-rock xenoliths, and tiny immiscible sulfide droplets in a dynamic stream of rising magma through a crustal conduit.

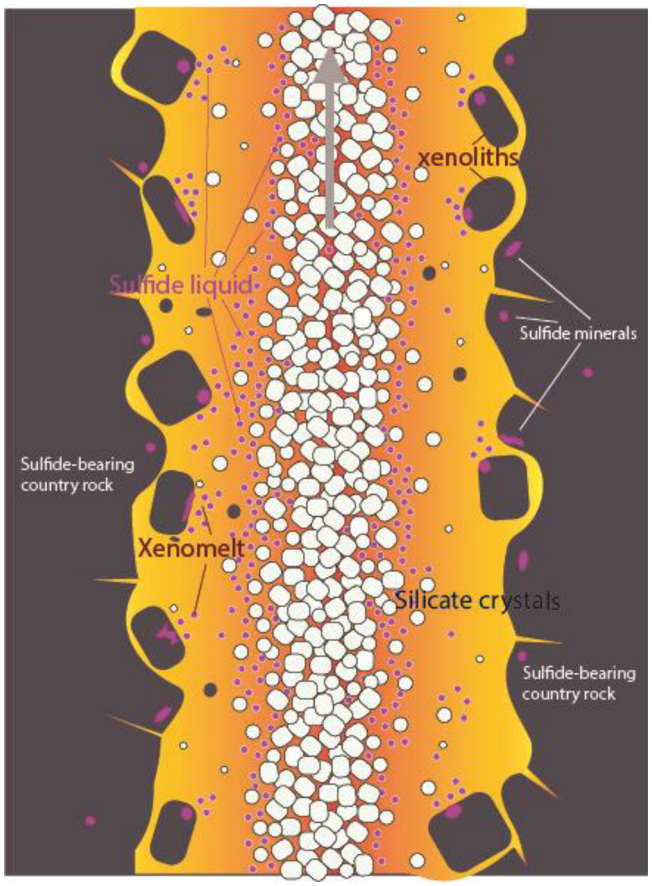

Fig. 8. A schematic diagram of magma flow in a conduit system through a S-rich country rocks. In the vertical flow direction of magma there is a large volume of silicate and oxide crystals which aggregate along the central portion of the conduit. Country rock fragments break into the magma by thermal and mechanical erosion. These xenoliths, upon melting, release sulfide "xenomelts" into the flowing magma. The tiny sulfide xenomelt droplets do not coalesce but move in unison with the crystal mush, even though at different velocities. The moving crystals churn the sulfide liquid droplets along the flow path. During flow in the conduit new sulfide xenomelts join with the already existing immiscible sulfide droplets in the magma.

6. Homogeneous mixing of the immiscible sulfide liquid was also caused by a gravity-driven downward displacement, upon the cessation of active magmatic transport in the conduit.

Acknowledgement

We are extremely thankful to Eagle Mine for providing financial support to this project. We are grateful to Bob Mahin, Espree Essig, Samantha Kleich, Mark DeHoog, Steve Beach and all other members of the exploration team for their assistance in drill core inspection, sample collection, preparation of 3D models and thoughtful discussions during this project. Melanie Humphrey of Michigan Department of Environmental Quality helped us in sampling drill core. Andrew Sasso participated in sample collection and during field trips. Discussions with Ed Ripley and Dean Rossell were extremely valuable. Useful suggestions by Mark Frank and an anonymous reviewer helped us to improve the quality of the article substantially. Associate editor, Jane Hammarstrom was very helpful during the editorial handling of the manuscript. Robb Gillespie and R.V. Krishnamurthy provided useful feedback in the early phase of the work.

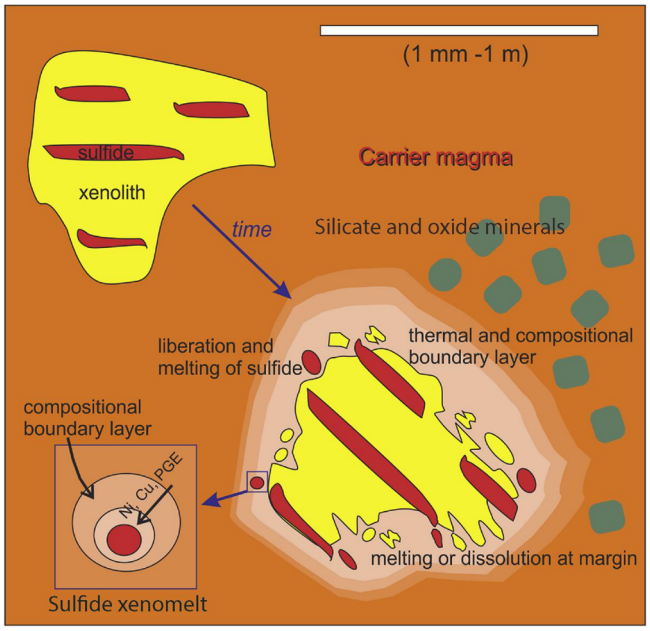

Fig. 9. A schematic figure showing the liberation of sulfide liquid from the margins of melting xenolith in a magma (from Barnes and Robertson, 2019). The sulfide liquid droplets equilibrate with the magma by absorption of chalcophile elements: Cu, Ni and PGE.

Appendix A. Supplementary data

Supplementary data to this article can be found online at https://doi.org/10.1016/j.oregeorev.2019.01.008.

References

Arndt, N.T., Lesher, C.M., Czamanske, G.K., 2005. Mantle-derived Magmas and Magmatic Ni-Cu-(PGE) Deposits, 100th Anniversary Volume. Society of Economic Geologists, pp. 5–23.

Barnes, S.J., Le Vaillant, M., Lightfoot, P.C., 2017. Textural development in sulfide matrix ore breccias and associated rocks in the Voisey's Bay Ni-Cu-Co deposit, Labrador, Canada. Ore Geol. Rev. 90, 414–438.

Barnes, S.-J., Lightfoot, P.C., 2005. Formation of magmatic nickel sulfide ore deposits and processes affecting their copper and platinum group element contents. 100th Anniversary Volume. Society of Economic Geologists, pp. 179–214.

Barnes, S.J., Robertson, J.C., 2019. Time scales and length scales in magma flow pathways and the origin of magmatic Ni-Cu-PGE ore deposits. Geosci. Front. 10, 77–87.

Barnes, S.J., Cruden, A.R., Arndt, N., Saumur, B.M., 2016. The mineral system approach applied to magmatic Ni–Cu–PGE sulphide deposits. Ore Geol. Rev. 76 (2016), 296–316.

Benson, E., Ripley, E.M. and Li, V. (2018) Sulfur isotope heterogeneity in disseminated sulfide mineralization: Insights from the East Eagle deposit, northern Michigan, Geological Society of America Abstracts with Programs. Vol. 50, No. 6, doi: 10.1130/abs/2018AM-318573.

Bhattacharji, S., Smith, C.H., 1964. Flowage differentiation. Science 145, 150–153.

Brügmann, G.E., Naldrett, A.J., Asif, M., Lightfoot, P.C., Gorbachev, N.S., Fredorenko, V.A., 1993. Siderophile and chalcophile metals as tracers of the evolution of the Siberian Trap in the Noril'sk region, Russia. Geochim. Cosmochim. Acta 57, 2001–2018.

Buchanan, D.I., Nolan, J., 1979. Solubility of sulfur and sulfide immiscibility in synthetic tholeiitic melts and their relevance to Bushveld Complex rocks. Can. Mineral. 17, 483–494.

Campbell, I.H., Naldrett, A.J., 1979. The influence of silicate: sulfide ratios on the

geochemistry of magmatic sulphides. Econ. Geol. 74, 1503–1506.
Clow, G.G., Lecuyer, N.L., Rennie, D.W., Scholey, B.J.Y., 2017. Technical Report on the Eagle Mine, Michigan, USA. Lundin Mining Corporation, pp. 306.
Correa-Gomes, L.C., Filho, C.R.S., Martins, C.J.F.N., Oliveira, E.P., 2001. Development of symmetrical and asymmetrical fabrics in sheet-like igneous bodies: the role of magma flow and wall-rock displacements in theoretical and natural cases. J. Struct. Geol. 23, 1415–1428.
Ding, X., Li, C., Ripley, E.M., Rossell, D., Kamo, S., 2010. The Eagle and East Eagle sulfide ore-bearing mafic–ultramafic intrusions in the Midcontinent Rift System, Upper Michigan: geochronology and petrologic evolution. Geochem. Geophys. Geosyst. https://doi.org/10.1029/2009GC002546.
Ding, X., Li, C., Ripley, E.M., Li, C., 2011. PGE geochemistry of the Eagle Ni-Cu-PGE deposit, Upper Michigan: constraints on ore genesis in a dynamic magma conduit. Miner. Deposita 47, 89–104.
Ding, X., Li, C., Ripley, E.M., Shirey, S.B., Li, C., 2012. Os, Nd, O and S isotope constraints on country rock contamination in the conduit-related Eagle Cu–Ni–(PGE) deposit, Midcontinent Rift System, Upper Michigan. Geochim. Cosmochim. Acta 89, 10–30.
Fiorentini, M., Beresford, S., Barley, M., Duuring, P., Bekker, A., Rosengren, N., Cas, R., Hronsky, J., 2012. District to camp controls on the genesis of komatiite-hosted nickel sulfide deposits, Agnew-Wiluna Greenstone Belt, Western Australia: insights from the multiple sulfur isotopes. Econ. Geol. 107, 781–796.
Gaetani, G.A., Grove, T.L., 1999. Wetting of mantle olivine by sulfide melt: Implications for Re/Os ratios in mantle peridotite and late – stage core formation, Earth Planet. Sci. Lett. 169, 147–163.
Gorbachev, N.S., Grinenko, L.N., 1973. The sulfur-isotope ratios of the sulfides and sulfates of the Oktyabr'sky sulfide deposit, Noril'sk region, and the problem of its origin. Geokhimiya 8, 1127–1136.
Grinenko, L.N., 1985. Sources of sulfur of the nickeliferous and barren gabbro-dolerite intrusions of the northwest Siberian platform. Int. Geol. Rev. 28, 695–708.
Holwell, D.A., Boyce, A.J., McDonald, I., 2007. Sulfur isotope variation within the Platreef Ni-Cu-PGE deposit: genetic implications for the origin of sulfide mineralization. Econ. Geol. 102, 1091–1110.
Holwell, D.A., Abraham-James, T., Keays, R.R., Boyce, A.J., 2012. The nature and genesis of marginal Cu–PGE–Au sulphide mineralisation in Paleogene Macrodykes of the Kangerlussuaq region, East Greenland. Mineral. Deposita 47, 3–21.
Hughes, H.S.R., McDonald, I., Boyce, A.J., Holwell, D.A., Kerr, A.C., 2016. Sulphide sinking in magma conduits: evidence from mafic-ultramafic plugs on rum and the wider North Atlantic Igneous Province. J. Petrol. 57, 383–416.
Irvine, T.N., 1975. Crystallization sequences of the Muskox intrusion and other layered intrusions: II. Origin of the chromite layers and similar deposits of other magmatic ores. Geochim. Cosmochim. Acta 39, 991–1020.
Johnson, R.C., Bornhorst, T.J., 1991. Archean Geology of the Northern Block of the Ishpeming Greenstone Belt, Marquette Country, Michigan. U.S Geological Survey Bulletin, pp. 20 1904-F.
Keays, R.R., Lightfoot, P.C., 2010. Crustal sulfur is required to form magmatic Ni-Cu sulfide deposits: evidence from chalcophile element signatures of Siberian and Deccan Trap basalts. Miner. Deposita 45, 241–257.
Kerr, A., Leitch, A.M., 2005. Self-destructive sulfide segregation systems and the formation of high-grade magmatic ore deposits. Econ. Geol. 100, 311–332.
Komar, P.O., 1976. Phenocryst interactions and the velocity profile of magma flowing through dikes and sills. Geol. Soc. Am. Bull. 87, 1336.
Lambert, D.D., Foster, J.G., Frick, L.R., Ripley, E.M., Zientek, M.L., 1998. Geodynamics of magmatic Cu–Ni–PGE sulfide deposits: new insights from the Re–Os isotope system. Econ. Geol. 93, 121–133.
Lehmann, J., Arndt, N., Windley, B., Zhou, M.F., Wang, C.Y., Harris, C., 2007. Field relationships and geochemical constraints on the emplacement of the Jinchuan intrusion and its Ni–Cu–PGE sulfide deposit, Gansu. China. Econ. Geol. 102, 75–94.
Lesher, C.M., 2017. Roles of xenomelts, xenoliths, xenocrysts, xenovolatiles, residues, and skarns in the genesis, transport, and localization of magmatic Fe-Ni-Cu-PGE sulfides and chromite. Ore Geol. Rev. 90, 465–484.
Lesher, C.M., 2018. The rise and fall of magmatic Ni-Cu-PGE sulfides. Geological Society of America Abstracts with Programs. Vol. 50, No. 6, doi: 10.1130/abs/2018AM-321594.
Lesher, C.M., Arndt, N.T., Groves, D.I., 1984. Genesis of komatiite-associated nickel sulphide deposits at Kambalda, Western Australia: a distal volcanic model. In: Buchanan, D.L., Jones, M.J. (Eds.), Sulphide Deposits in Mafic and Ultramafic Rocks. Institution of Mining and Metallurgy, London, pp. 70–80.
Lesher, C.M., Groves, D.I., 1986. Controls on the formation of komatiite-associated nickel–copper sulfide deposits. In: Friedrich, G.H., Genkin, A.D., Naldrett, A.J. (Eds.), Geology and Metallogeny of Copper Deposits. Springer, pp. 43–62.
Li, C., Naldrett, A.J., 2000. Melting reactions of gneissic inclusions with enclosing magma at Voisey's Bay, Labrador, Canada; implications with respect to ore genesis. Econ. Geol. Bull. Soc. Econ. Geol. 95, 801–814.
Li, C., Ripley, E.M., 2005. Empirical equations to predict the sulfur content of mafic magma at sulfide saturation and applications to magmatic sulfide deposits. Mineral. Deposita 40, 218–230.
Lightfoot P.C., Hawkesworth C.J., 1997. Flood basalts and magmatic Ni, Cu, and PGE sulphide mineralization: Comparative geochemistry of the Noril'sk (Siberian Traps) and West Greenland Sequences. In: Large Igneous Provinces, vol. 100 (eds. J. J. Mahoney and M. F. Coffin). Am. Geophys. Union Mon., pp. 357–380.
Lightfoot, P.C., Evans-Lamswood, D.M., 2015. Structural controls on the primary distribution of mafic-ultramafic intrusions containing Ni-Cu-Co-(PGE) sulfide mineralization in the roots of large igneous provinces. Ore Geol. Rev. 64, 354–386.
Lightfoot, P.C., Keays, R.R., 2005. Siderophile and chalcophile metal variations in flood basalts from the Siberian Trap, Noril'sk Region: Implications for the origin of the Ni-Cu-PGE sulfide ores. Econ. Geol. 100, 439–462.
Li, C., Ripley, E.M., Naldrett, A.J., 2003. Compositional variations of olivine and sulfur isotopes in the Noril'sk and Talnakh intrusions, Siberia: Implications for ore forming processes in dynamic magma conduits. Econ. Geol. 98, 69–86.
Lightfoot, P.C., Keays, R.R., Evans-Lamswood, D., Wheeler, R., 2012. S saturation history of Nain plutonic suite mafic intrusions; origin of the Voisey's Bay Ni-Cu-Co sulfide deposit, Labrador, Canada. Miner. Deposita 47, 23–50.
Lundin Mining, 2016. Lundin Mining Announces Eagle East Mineral Resource, PEA Results and Project Commencement; https://lundinmining.com/news/lundin-mining-announces-eagle-east-mineral-resourc-122539/; News release, June 29, 2016.
Maier, W., Barnes, S.J., Sarkar, A., Ripley, E.M., Li, C., Livesey, T., 2010. The Kabanga Ni sulfide deposit, Tanzania: I. Geology, petrography, silicate rock geochemistry, and sulfur and oxygen isotopes. Mineral. Deposita 45, 419–441.
Mavrogenes, J.A., O'Neil, H., 1999. The relative effects of pressure, temperature and oxygen fugacity on the solubility of sulphide in mafic magmas. Geochim. Cosmochim. Acta 63, 1173–1180.
McLeod, P., Sparks, R.S.J., 1998. The dynamics of xenolith assimilation. Contrib. Miner. Petrol. 132, 21–33.
Mungall, J.E., Su, S., 2005. Interfacial tension between magmatic sulfide and silicate liquids: constraints on kinetics of sulfide liquation and sulfide migration through silicate rocks. Earth Planet. Sci. Lett. 234, 135–149.
Naldrett, A.J., 1999. World-class Ni-Cu-PGE deposits: key factors in their genesis. Miner. Deposita 34, 227–240.
Naldrett, A.J., 2004. Magmatic Sulfide Deposits: Geology, Geochemistry and Exploration. Springer, Heidelberg, pp. 727.
Naldrett, A.J., Fedorenko, V.A., Lightfoot, P.C., Kunilov, V.E., Gorbachev, N.S., Doherty, W., Johan, Z., 1995. Ni-Cu-PGE deposits of the Noril'sk region, Siberia: their formation in conduits for flood basalt volcanism. Trans. Instit. Mining Metall. 104, B18–B36.
Naldrett, A.J., Lightfoot, P.C., 1993. A model for giant magmatic sulfide deposits associated with flood basalts. Econ. Geol. Spec. Pub. 2, 81–124.
Nicholson, S.W., Shirey, S.B., Schulz, K.J., Green, J.C., 1997. Rift-wide correlation of 1.1 Ga MRS basalts: implications for multiple mantle sources during rift development. Can. J. Earth Sci. 34, 504–520.
Penniston-Dorland, S.C., Wing, B.A., Nex, P.A.M., Kinnaird, J.A., Farquhar, J., Brown, M., Sharman, E.R., 2008. Multiple sulfur isotopes reveal a magmatic origin for the Platreef platinum group element deposit, Bushveld Complex, South Africa. Geology 36, 979–982.
Peterman, Z.E., Zartman, R.E., Sims, P.K., 1980. Gneiss of early Archean age in northern Michigan, U.S.A. Inst. Lake Superior Geol. 26, 332–334.
Ripley, E.M., Li, C., 2003. Sulfur isotope exchange and metal enrichment in the formation of magmatic Cu–Ni–(PGE) deposits. Econ. Geol. 98, 635–641.
Ripley, E.M., Li, C., 2013. Sulfide saturation in mafic magmas: is external sulfur required for magmatic Ni-Cu-(PGE) ore genesis? Econ. Geol. 108, 45–58.
Ripley, E.M., Li, C., 2017. A review of the application of multiple isotopes to magmatic Ni-Cu-PGE deposits and the significance of spatially variable $\Delta^{33}S$ values. Econ. Geol. 112, 983–991.
Ripley, E.M., Park, Y., Li, C., Naldrett, A.J., 1999. Sulfur and oxygen isotopic evidence of country rock contamination in the Voisey's Bay Ni–Cu–Co deposit, Labrador, Canada. Lithos 47, 53–68.
Ripley, E.M., Li, C., Shin, D., 2002. Paragneiss assimilation in the genesis of magmatic Ni-Cu-Co sulfide mineralization at Voisey's Bay, Labrador: $\delta^{34}S$, $\delta^{13}C$, and Se/S evidence. Econ. Geol. 97, 1307–1318.
Ripley, E.M., Lightfoot, P.C., Li, C., Elswick, E.R., 2003. Sulfur isotopic studies of continental flood basalts in the Noril'sk region: Implications for the association between lavas and ore-bearing intrusions. Geochimica et Cosmochimica Acta 67, 2805–2817.
Ripley, E.M., Sarkar, A., Li, C., 2005. Mineralogic and stable isotope studies of hydrothermal alteration at the Jinchuan Ni-Cu deposit, China. Econ. Geol. 100, 1349–1361.
Ripley, E.M., Li, C., Moore, C.H., Schmitt, A.K., 2010. Micro-scale S isotope studies of the Kharaelakh intrusion, Noril'sk region, Siberia: constraints on the genesis of coexisting anhydrite and sulfide minerals. Geochim. Cosmochim. Acta 74, 634–644.
Ripley, E.M., Dong, S., Li, C., Wasylenki, L.E., 2015. Cu isotope variations between conduit and sheet-style Ni–Cu–PGE sulfide mineralization in the Midcontinent Rift System, North America. Chem. Geol. 414, 59–68.
Robertson, J.C., Barnes, S.J., Le Vaillant, M., 2016. Dynamics of magmatic sulphide droplets during transport in silicate melts and implications for magmatic sulphide ore formation. J. Petrol. 56, 2445–2472.
Robertson, J., Ripley, E.M., Barnes, S.J., Li, C., 2015. Sulfur liberation from country rocks and incorporation in mafic magmas. Econ. Geol. 110, 1111–1123.
Ross, M.E., 1986. Flow differentiation, phenocryst alignment, and compositional trends within a dolerite dike at Rockport, Massachusetts. Geol. Soc. Am. Bull. 97, 232–240.
Rossell, D., Coombes, S., 2005. The geology of the Eagle nickel–copper deposit Michigan.

Kennecott Exploration report to Kennecott Minerals Company, USA, pp. 34.
Samalens, N., Barnes, S.-J., Sawyer, E.J., 2017. The role of black shales as a source of sulfur and semimetals in magmatic nickel-copper deposits: example from the Partridge River Intrusion, Duluth Complex, Minnesota, USA. Ore Geol. Rev. 81, 173–187.
Schneider, D.A., Bickford, M.E., Cannon, W., Schulz, K., Hamilton, M., 2002. Age of volcanic rocks and syndepositional iron formations. Marquette Range Supergroup: implications for the tectonic setting of Paleoproterozoic iron formations of the Lake Superior region. Can. J. Earth Sci. 39, 999–1012.
Schulz, K.J., Cannon, W.F., 2007. The Penokean orogeny in the Lake Superior region. Precambr. Res. 157, 4–25.
Seat, Z., Beresford, S.W., Grguric, B.A., Gee, M.A.M., Grassineau, N.V., 2009. Reevaluation of the role of external sulfur addition in the genesis of Ni-Cu-PGE deposits: Evidence from the Nebo-Babel Ni-Cu-PGE deposit, West Musgrave, Western Australia. Econ. Geol. 104, 521–538.
Sharman, E.R., Penniston-Dorland, S.C., Kinnaird, J.A., Nex, P.A.M., Brown, M., Wing, B.A., 2013. Primary origin of marginal Ni-Cu-(PGE) mineralization in layered intrusions: $\Delta^{33}S$ evidence from the Platreef, Bushveld, South Africa. Econ. Geol. 108, 365–377.
Sims, P.K., 1991. Great Lakes Tectonic Zone in Marquette Area, Michigan – implications for Archean Tectonics in North-Central United States. U.S. Geol. Surv. Bull. 1904-E, E1–E17.
Sims, P.K., Anderson, J.L., Bauer, R.L., Chandler, V.W., Hanson, G.N., Kalliokoski, J., Morey, J.B., 1993. The Lake Superior region and Trans-Hudson orogen, Precambrian: conterminous U.S. The Geology of North America. The Geological Society of America, Boulder, CO, pp. 11–122.
Sims, P.K., 1992. Geologic map of Precambrian rocks, southern Lake Superior region, Wisconsin and northern Michigan reports, U.S. Geological Survey, Miscellaneous Investigations Series Map I-2185, Map scale: 1:500,000.
Stein, S., Stein, C.A., Elling, R., Kley, J., Keller, G.R., Wysession, M., Rooney, T., Fredriksen, A., Moucha, R., 2018. Insights from North America's failed Midcontinent Rift into the evolution of continental rifts and passive continental margins. Tectonophysics 744, 403–421.
Studley, S.A., Ripley, E.M., Elswick, E.R., Dorais, M.J., Fong, J., Finkelstein, D., Pratt, L.M., 2002. Analysis of sulfides in whole rock matrices by elemental analyzer-continuous flow isotope ratio mass spectrometry. Chem. Geol. 192, 141–148.
Taranovic, V., Ripley, E.M., Li, C., Rossell, D., 2016. Chalcophile element (Ni, Cu, PGE, and Au) variations in the Tamarack magmatic sulfide deposit in the Midcontinent Rift System: implications for dynamic ore-forming processes. Miner. Deposita 51, 937–951.
Thakurta, J., Ripley, E.M., Li, C., 2008. Geochemical constraints on the origin of sulfide mineralization in the Duke Island Complex, southeastern Alaska. Geochem. Geophys. Geosyst. 9, 34. https://doi.org/10.1029/2008GC001982. Q07003.
Tohver, E., Holm, D., van der Pluijm, B.A., Essene, E.J., Cambray, F.W., 2007. Late Paleoproterozoic (geon 18 and 17) reactivation of the Neoarchean Great Lakes Tectonic Zone, northern Michigan, USA: Evidence from kinematic analysis, thermobarometry and 40Ar/39Ar geochronology. Precambr. Res. 157, 144–168.
Van Schmus, W.R., Hinze, W.J., 1985. The Midcontinent Rift System. Ann. Rev. Earth Planet Sci. 13, 345–383.
Van Schmus, W.R., Woolsey, L.L., 1975. Rb–Sr geochronology of the Republic area, Marquette County, Michigan. Can. J. Earth Sci. 12, 1723–1733.
Van Schmus, W.R., Bickford, M.E., Zietz, I., 1987. Early and middle Proterozoic provinces in the central United States. In: Kroner, A. (Ed.), Proterozoic Lithosphere Evolution. Geodyn. Ser. AGU, Washington, DC vol. 17.